SAND2017-11041C

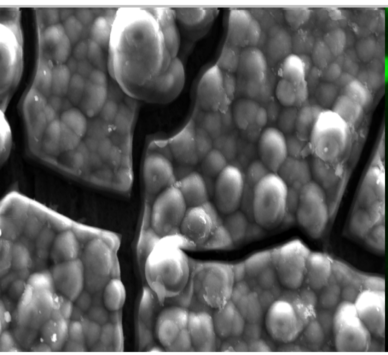
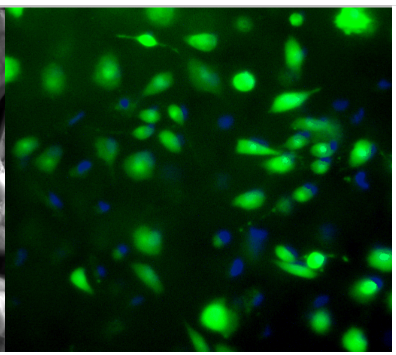
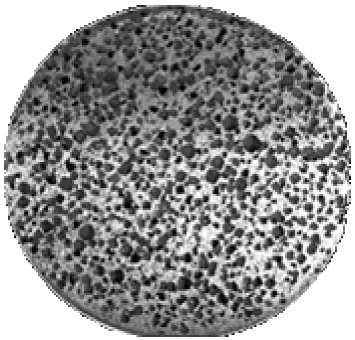
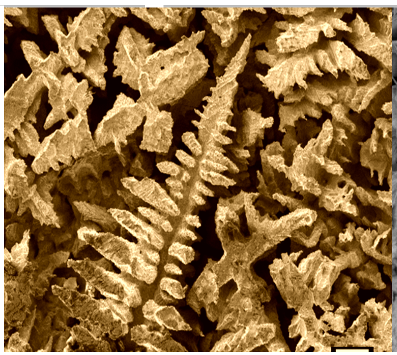
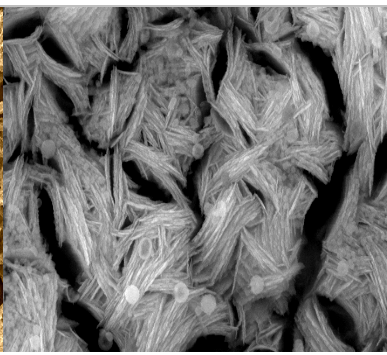

Porous Fe-Mn-Hydroxyapatite Composites and their Potential as Resorbable Implants

Michael Heiden, Lia Stanciu
Materials Engineering - Purdue University

Sandia National Laboratories is a multimission laboratory managed and operated by National Technology and Engineering Solutions of Sandia LLC, a wholly owned subsidiary of Honeywell International Inc. for the U.S. Department of Energy's National Nuclear Security Administration under contract DE-NA0003525.

Introduction to Resorbable Materials

- **Problem:** The presence of a permanent device may cause severe negative effects and require re-intervention and invasive procedures in the long-term
- **Bioresorbable Implant:** A transient device used to mechanically support the natural healing of injured or diseased tissue

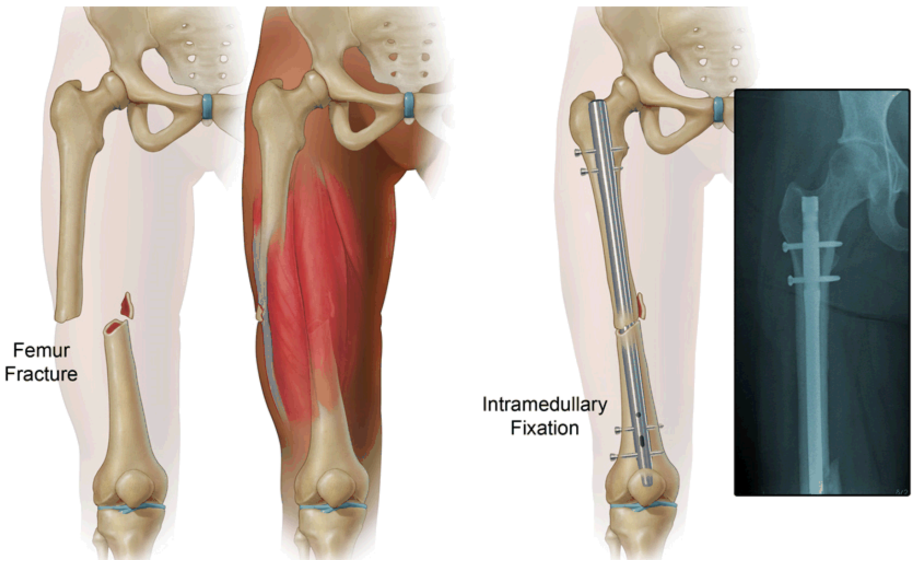

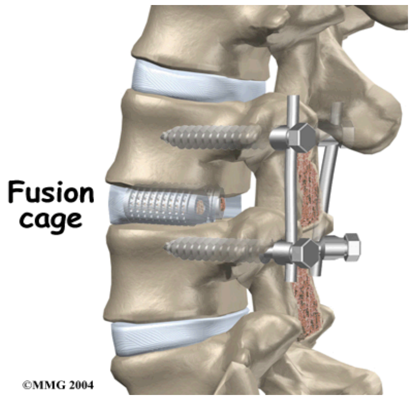

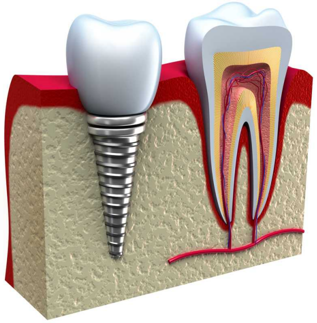

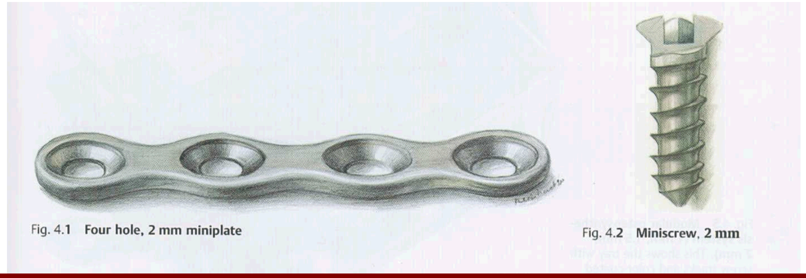

http://www.eorthopod.com/images/ContentImages/spine/spine_lumbar/lumbar_PLIF/lumbar_PLIF_rationale03.jpg
http://www.infinitydentalcare.com/websites/infinitydentalcarect/images/dental-implants.jpg
http://webdocs.cs.ualberta.ca/~database/MEMS/sma_mems/img/plate.jpg

Ideal Resorbable Material

Requirements

1) Be biocompatible and not cause local or systemic effects
2) Mechanically support full tissue healing and resorb in a timely manner
3) Encourage natural tissue attachment to prevent loosening
4) Release non-toxic degradation products

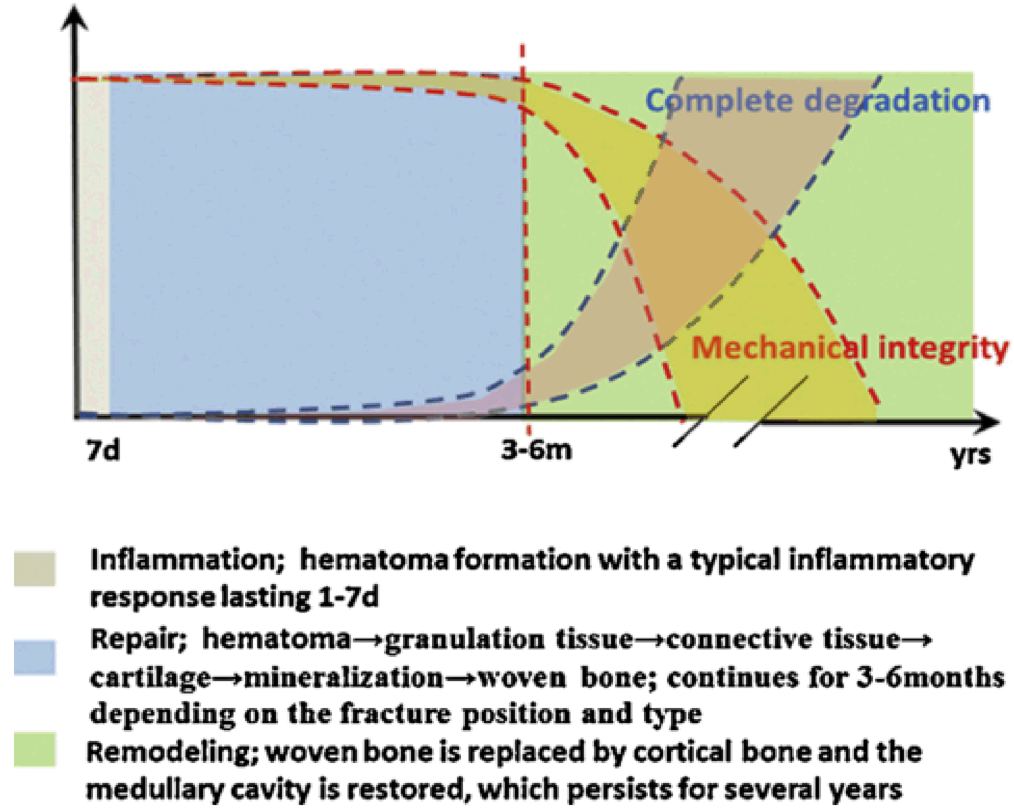

Biggest challenge: Tailoring the degradation rate

Zheng, Y. F.; Gu, X. N.; Witte, F. Biodegradable Metals. *Mater. Sci. Eng. R Reports* **2014**, *77*, 1–34.

Choosing a Metallic Material

Element	Human amount	Blood serum level	Pathophysiology	Toxicology	Daily allowance	Bone cell[d]	Vascular cell[d]
Essential nutrients							
Mg	25 g	0.73–1.06 mM	Activator of many enzymes; co-regulator of protein synthesis and muscle contraction; stabilizer of DNA and RNA	Excessive Mg leads to nausea	0.7 g	+	+
Fe	4–5 g	5.0–17.6 g/l	Component of several metalloproteins; be crucial in vital biochemical activities, i.e. oxygen sensing and transport	Iron toxicity gives rise to lesions in the gastrointestinal tract, shock and liver damage	10–20 mg	+–	+–
Ca	1100 g	0.919–0.993 mM	More than 99% has a structure function in the skeleton; the solution Ca has a signal function, including muscle contraction, blood clotting, cell function, etc.	Inhibit the intestinal absorption of other essential minerals	0.8 g	+	+
Zn	2 g	12.4–17.4 μM	Trace element; appears in all enzyme classes; most Zn appears in muscle	Neurotoxic and hinder bone development at higher concentration	15 mg	–	–
Mn	12 mg	<0.8 μg/l	Trace element; activator of enzyme; Mn deficiency is related to osteoporosis, diabetes mellitus, atherosclerosis	Excessive Mn results in neurotoxicity	4 mg	–	–
Potential essential metal							
Sr	0.3 g	0.17mg[a]	99% is located in bone; show dose dependent metabolic effect on bone; low doses stimulated new bone formation	High doses induce skeletal abnormalities	2 mg	+	+
Si	–	–	Cross linking agent of connective tissue; necessary for growth an bone calcification	Silica and silicate caused lung diseases	–		
Sn	30 mg	–	Tin-deficient diets in rat studies resulted in poor growth, reduced feeding efficiency, hearing loss, and bilateral (male) hair loss	Some organic compounds are poison, i.e. methyl and ethyl compounds	–	+–	+–
Other element							
Li	–	2–4 ng/g	Used in the treatment of manic-depressive psychoses	Plasma concentration of 2 mM is associated with reduced kidney function and neurotoxicity, 4 mM maybe fatal	0.1g[b]	+	+
Al	<300 mg	2.1–4.8 μg/l	–	Primarily accumulated in bone and nervous system; implicated Al in the pathogenesis of Alzheimer's disease	–	+	+
Zr	<250 mg		Probably excreted in feces; low systematic toxicity to animals	High concentration in liver and gall bladder	3.5 mg	+	+
Y and lanthanides		<47 μg[c]	Substituted for Ca^{2+} and matters when the metal ion at the active site; compound of drugs for treatment of cancer	Basic lanthanides deposited in liver; more acidic and smaller cations deposited in bone	–	+–	+–

Daily exposure limit for a 60-kg adult:

Fe: 2.55 mg/day
Mn: 0.42 mg/day

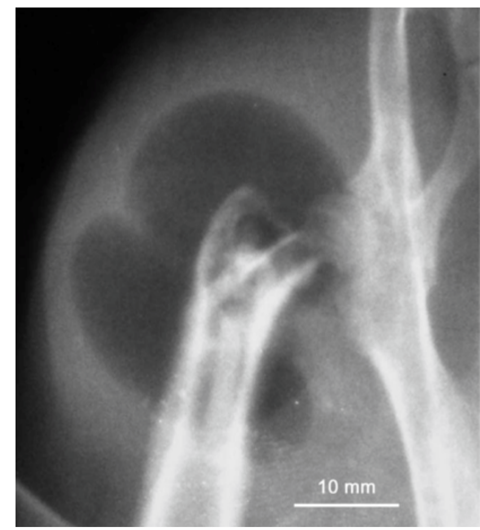

Yuen, C. K.; Ip, W. Y. Theoretical Risk Assessment of Magnesium Alloys as Degradable Biomedical Implants. *Acta Biomater.* **2010**, *6*, 1808–1812.
Zheng, Y. F.; Gu, X. N.; Witte, F. Biodegradable Metals. *Mater. Sci. Eng. R Reports* **2014**, *77*, 1–34.

90 Day Corrosion Study of Fe-Mn Alloys

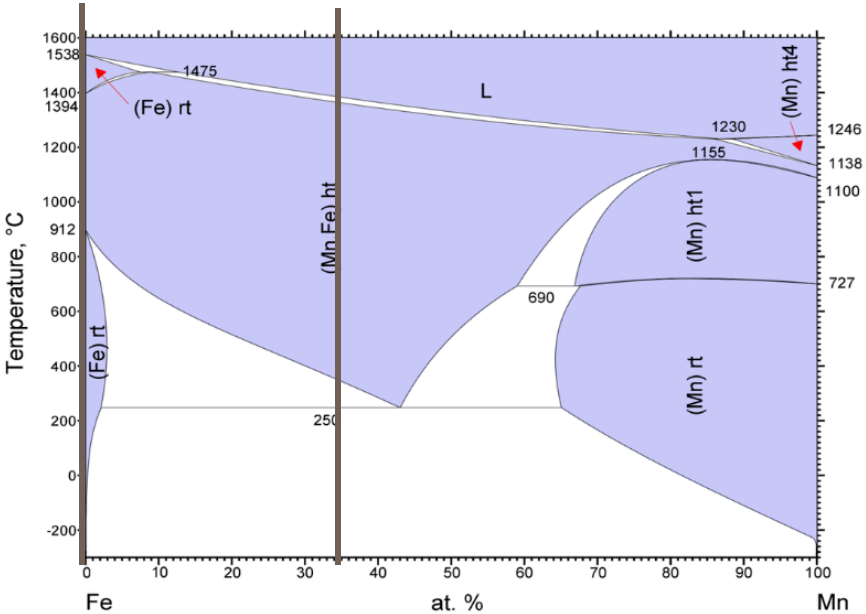

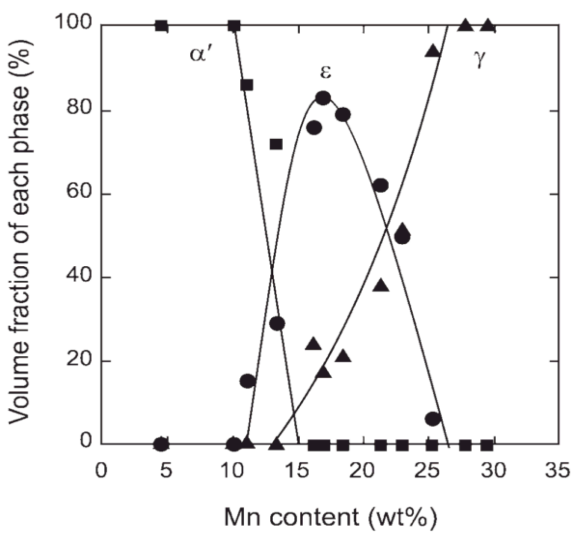

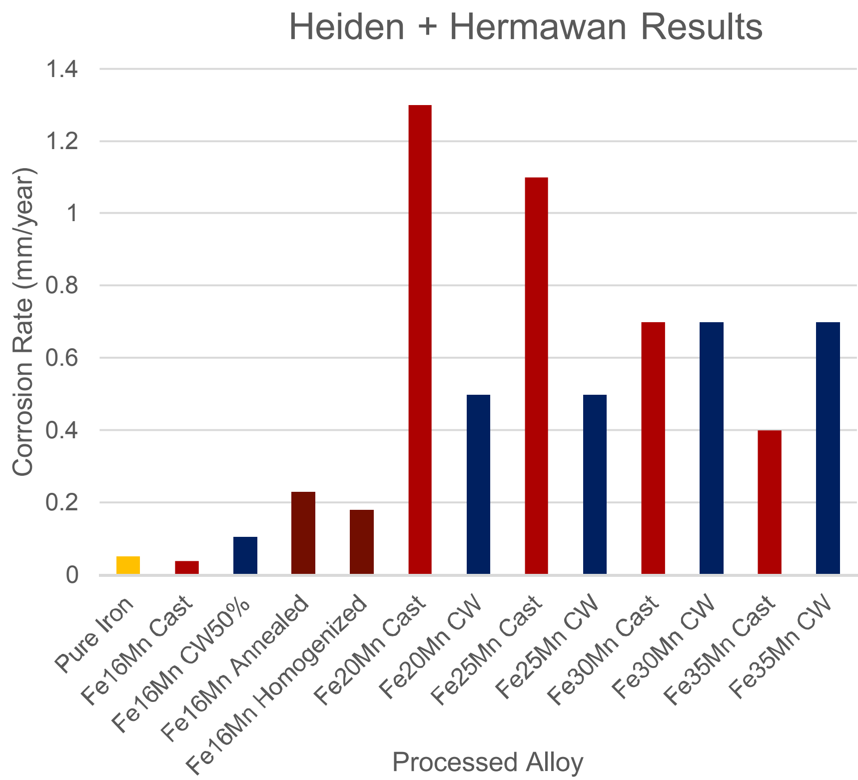

$$\mathrm{CR\ (mm/year)} = 3.27 \times 10^{3} \left(\frac{i_{corr} \times \mathrm{EW}}{D} \right)$$

$$\text{Corrosion rate (mm/year)} = \frac{K \times W}{A \times t \times D}$$

http://www1.asminternational.org/asmenterprise/APD/ViewAPD.aspx?id=100147

Hermawan, H.; Dubé, D.; Mantovani, D. Degradable Metallic Biomaterials: Design and Development of Fe-Mn Alloys for Stents. *J. Biomed. Mater. Res. A* **2010**, *93*, 1–11.

90 Day Corrosion Study of Fe-20Mn

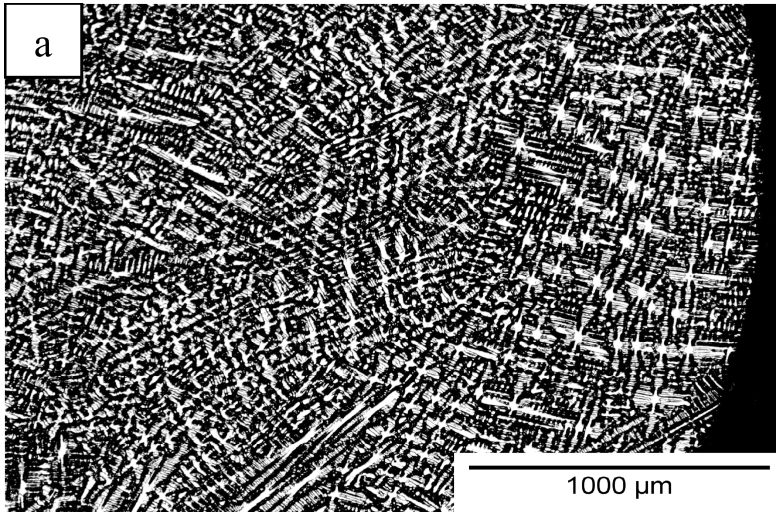

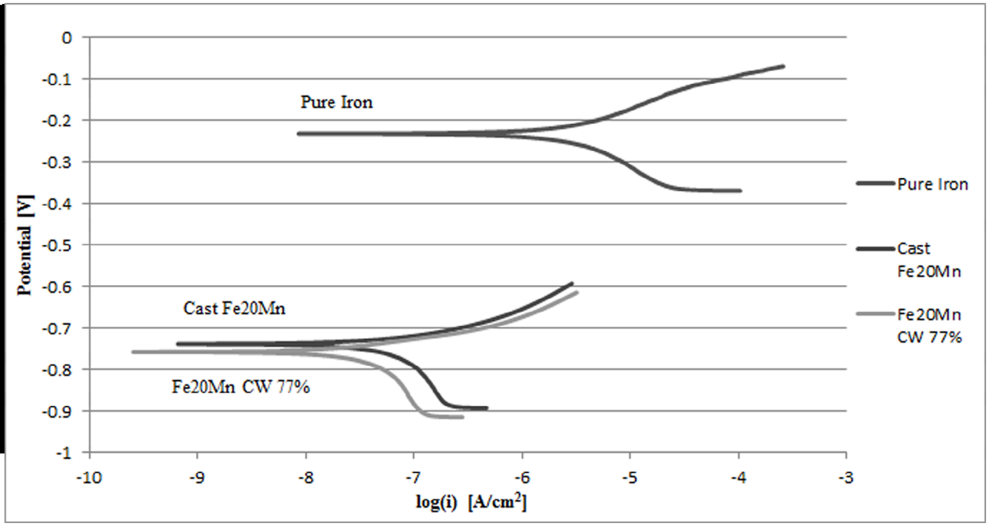

$(\text{CR} \sim 7 \times 10^{-9} \text{ mm/year})$,

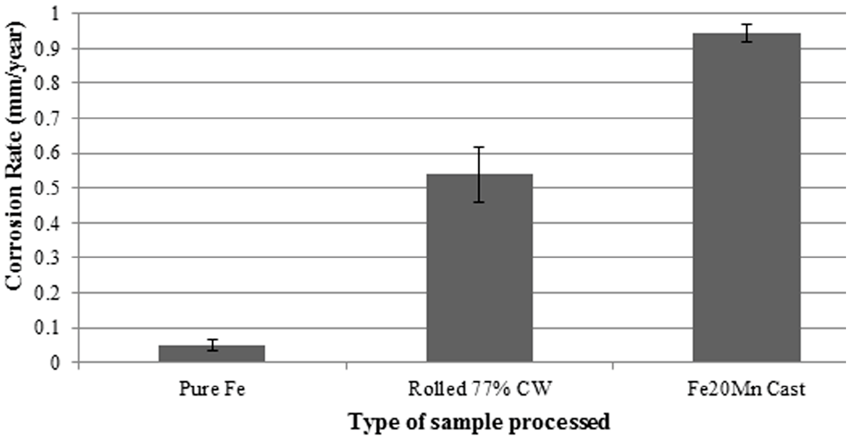

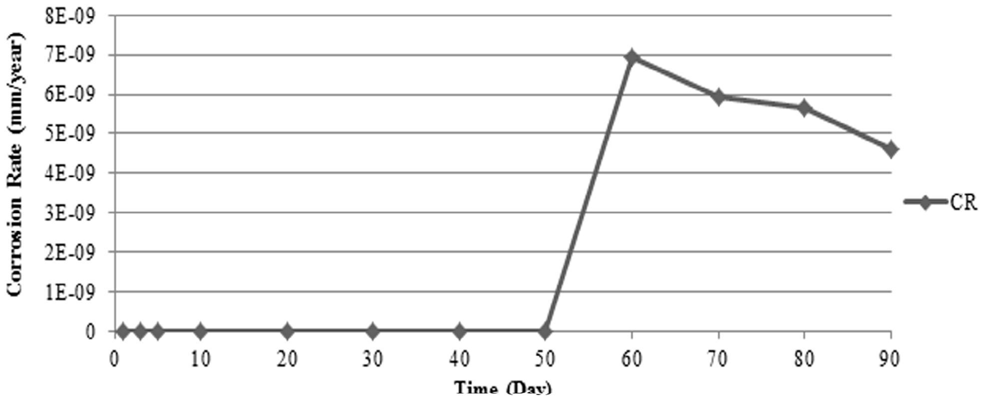

Heiden, M.; Walker, E.; Nauman, E.; Stanciu, L. Evolution of Novel Bioresorbable Iron-Manganese Implant Surfaces and Their Degradation Behaviors in Vitro. *J. Biomed. Mater. Res. A* **2014**, 1–9.

90 Day Corrosion Study of Fe-Mn Alloys

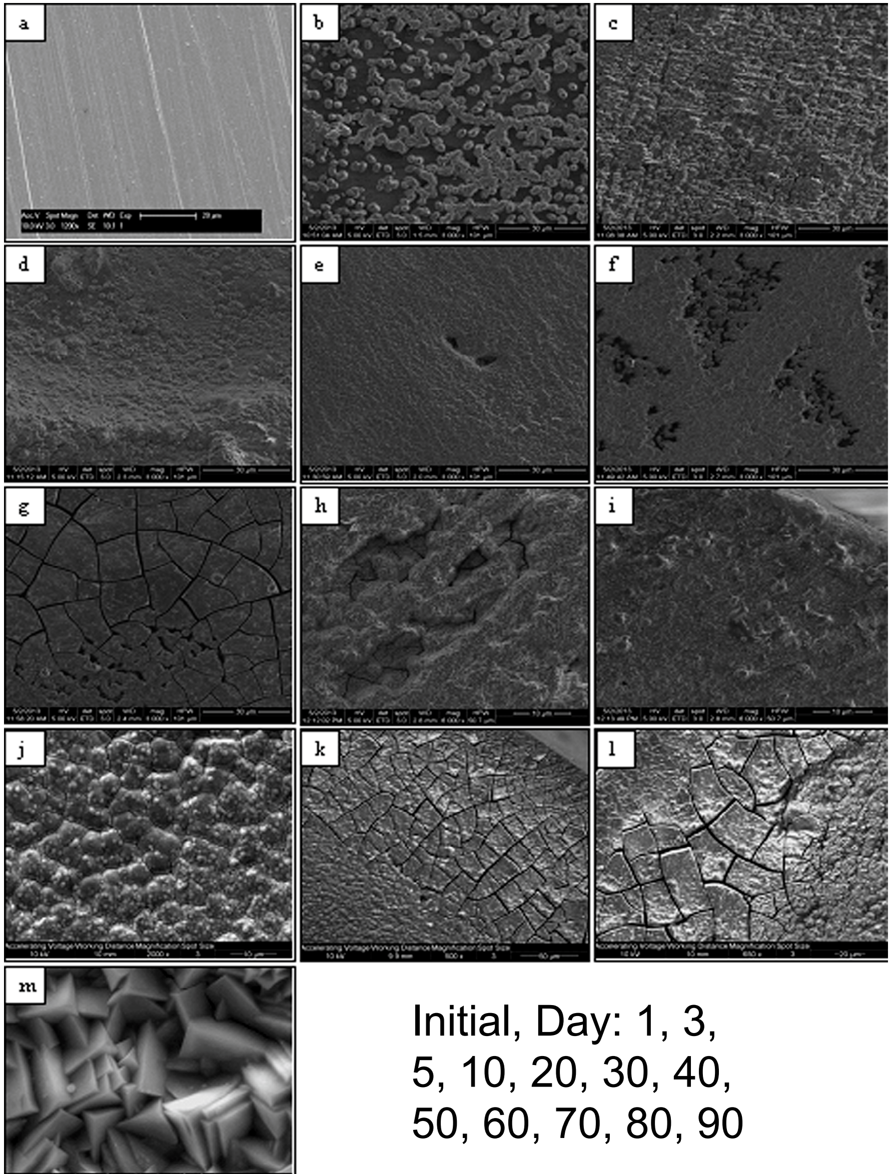

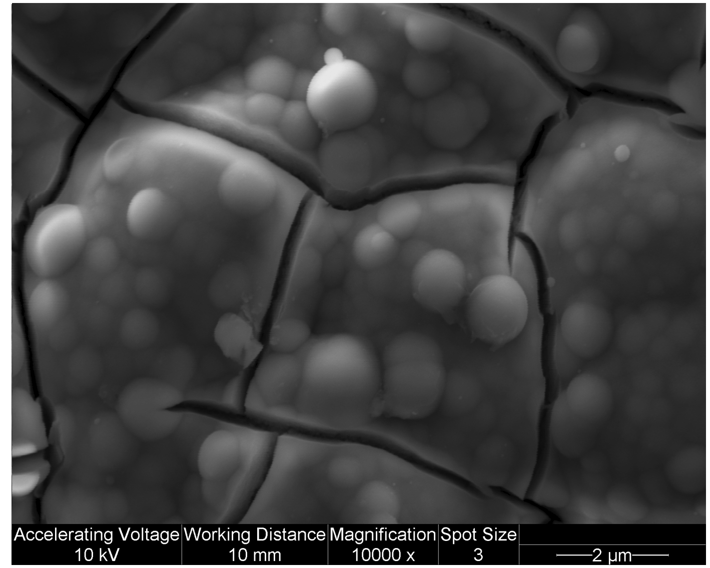

Initial, Day: 1, 3, 5, 10, 20, 30, 40, 50, 60, 70, 80, 90

Heiden, M.; Walker, E.; Nauman, E.; Stanciu, L. Evolution of Novel Bioresorbable Iron-Manganese Implant Surfaces and Their Degradation Behaviors in Vitro. *J. Biomed. Mater. Res. A* **2014**, 1–9.

90 Day Corrosion Study of Fe-Mn Alloys

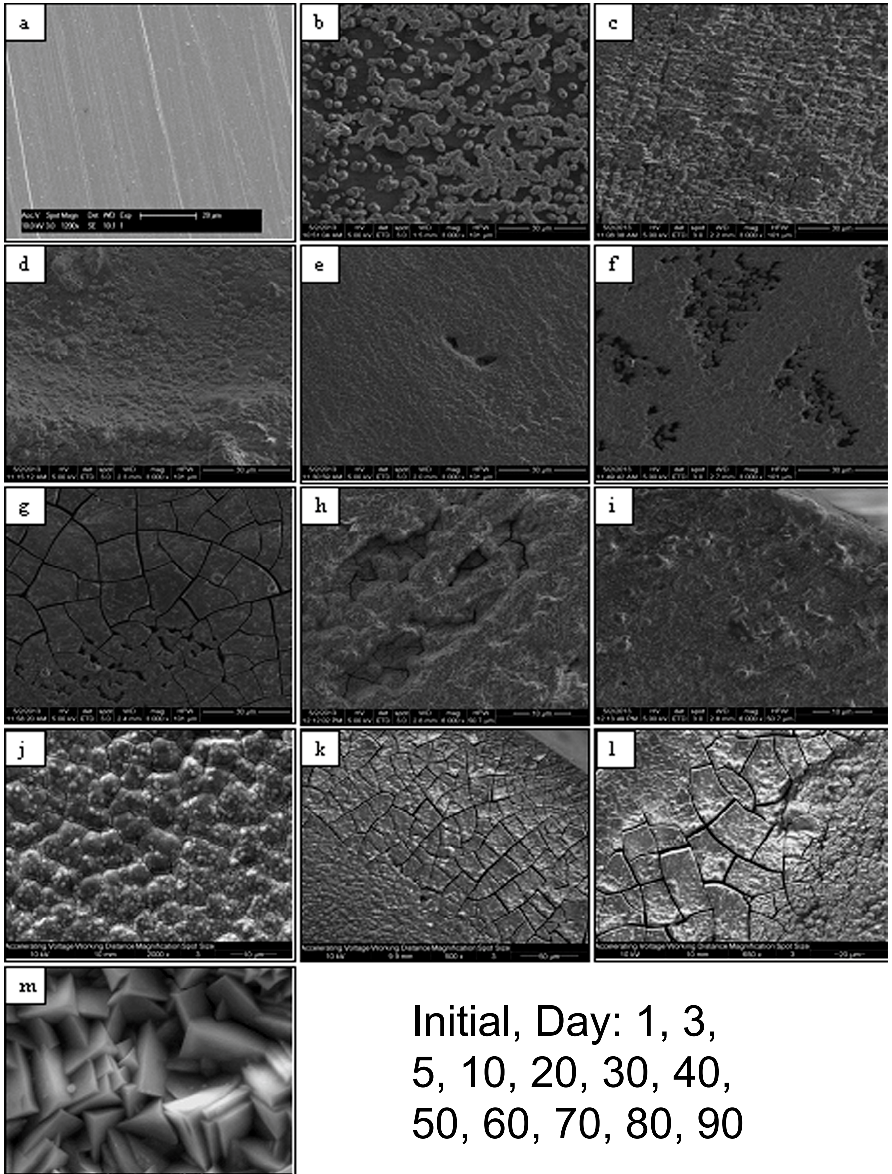

Initial, Day: 1, 3, 5, 10, 20, 30, 40, 50, 60, 70, 80, 90

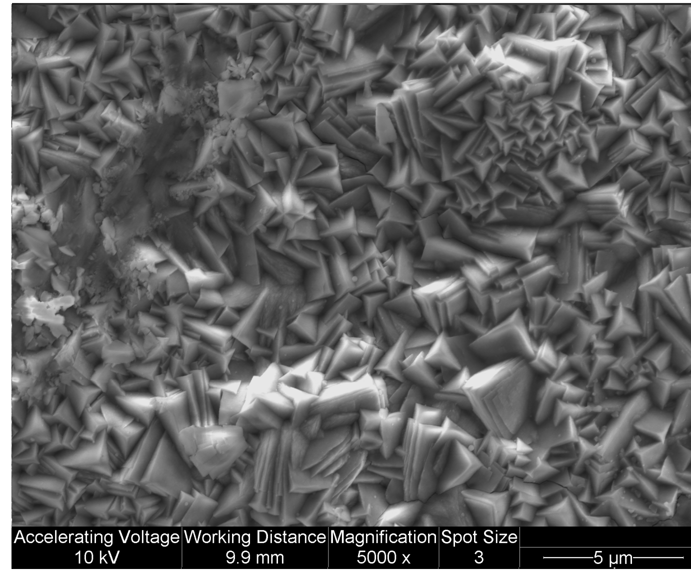

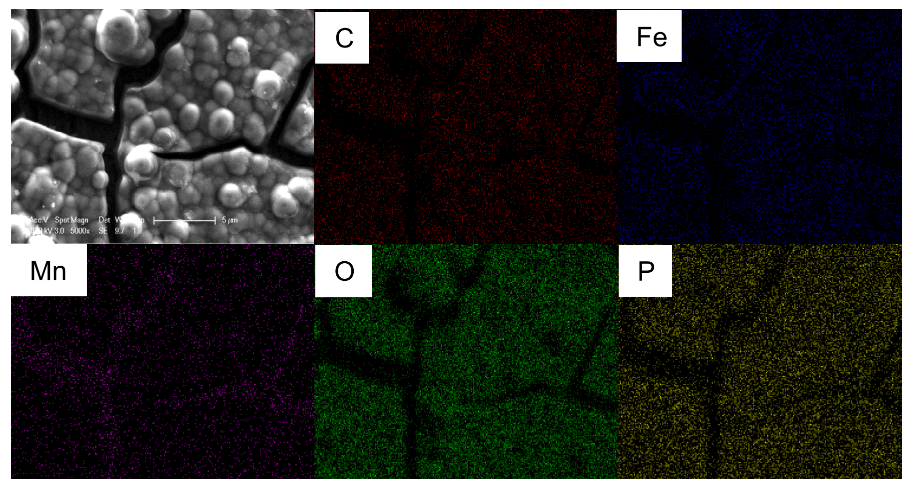

Heiden, M.; Walker, E.; Nauman, E.; Stanciu, L. Evolution of Novel Bioresorbable Iron-Manganese Implant Surfaces and Their Degradation Behaviors in Vitro. *J. Biomed. Mater. Res. A* **2014**, 1–9.

Six Month in vivo Rat Study of Fe-30Mn

Fe30Mn

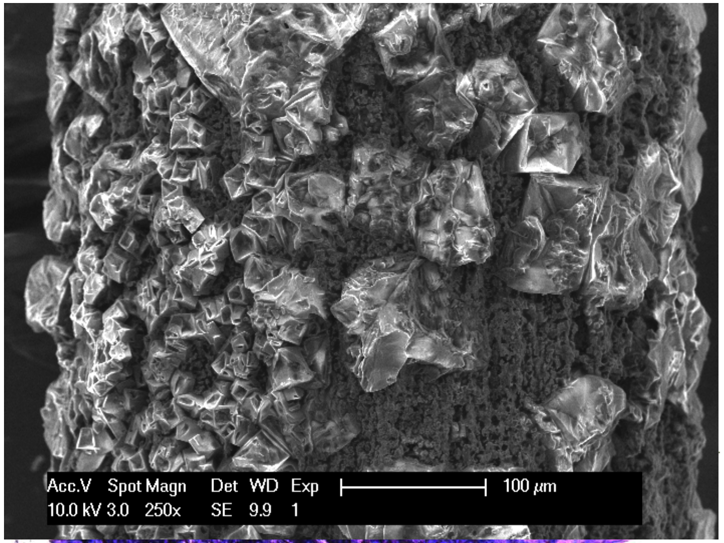

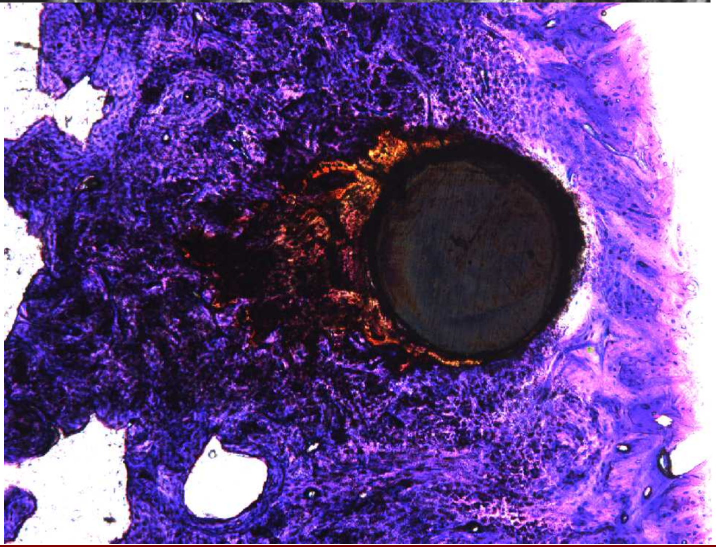

316 Stainless Steel

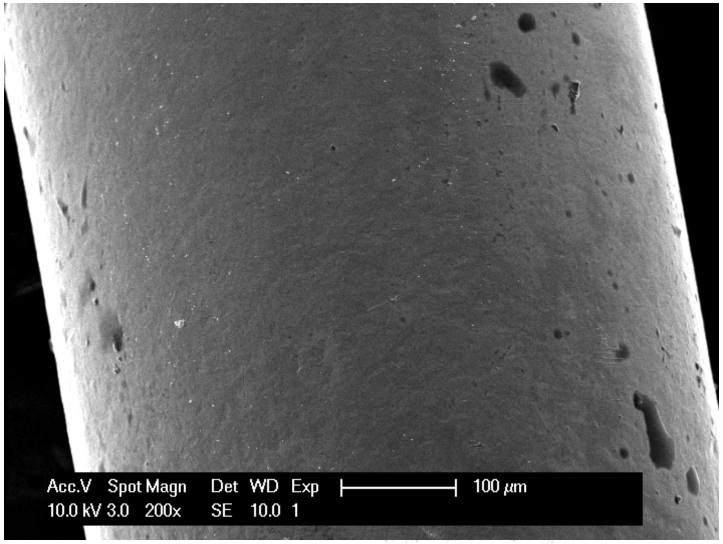

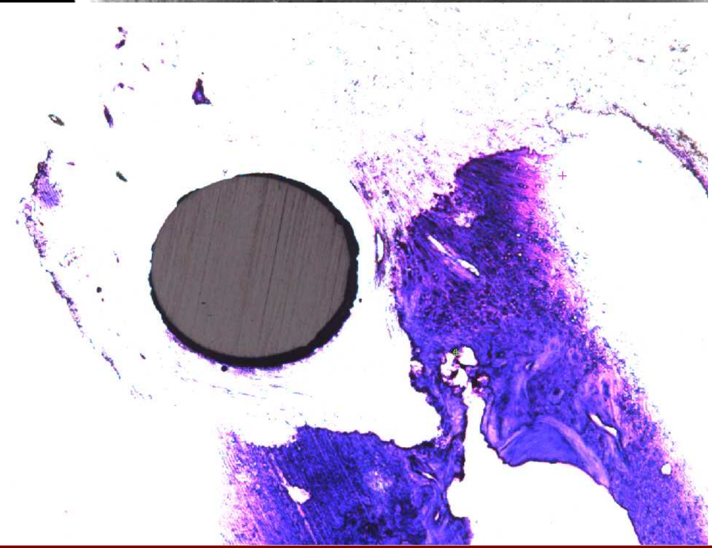

Experiment Design

Sandia National Laboratories

Variables

Alloy Composition

Microstructure

Surface Structures

Porosity

Other elements

Manufacturing Processes

- Powder Metallurgy
- Sintering
- NaCl-leaching
- Addition of Hydroxyapatite

Effects on Implant

Degradation

Cellular Attachment

Mechanical Properties

Long-term Biocompatibility

Microporous Structures through Leaching

Sandia National Laboratories

Variable factors include:

- Powder size, morphology, and purity
- Mixing
- Pressing load/pressure
- Sintering conditions
- Post-processing

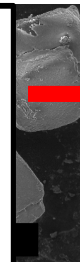
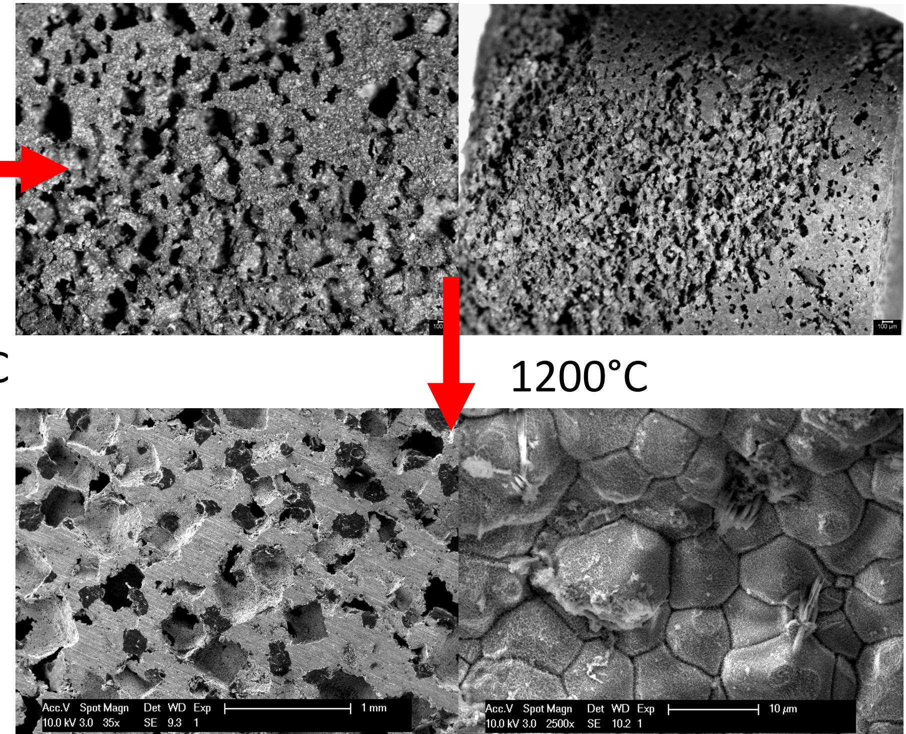

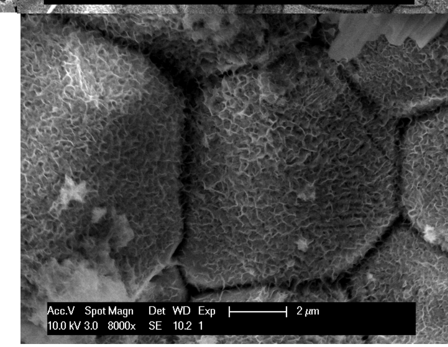

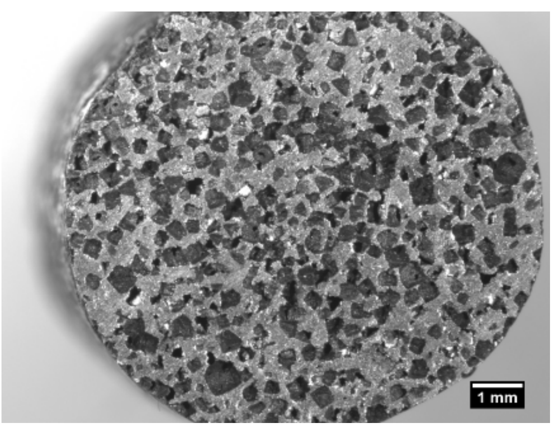

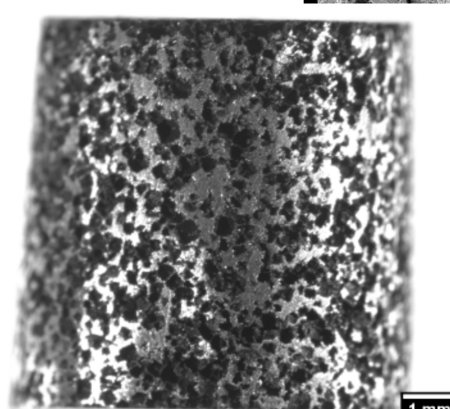

Heiden, M. Nauman E, Johnson D, Stanciu L. Bioresorbable Fe-Mn and Fe-Mn-HA Materials for Orthopedic Implantation: Enhancing Degradation through Porosity Control, *Adv. Healthcare* 6(13),10.1002/adhm.201700120 (2017)

Fe-Mn and Fe-Mn-HA Study

A. Fe30Mn (1200°C - 3hr)
B. 10% HA + Fe30Mn
C. 30% NaCl-leach (300µm)
D. 30% NaCl-leach (50µm)
E. 50% NaCl-leach (300µm)
F. 50% NaCl-leach (50µm)
G. 10%HA+30%NaCl-leach (300µm)
H. 10%HA+30%NaCl-leach (50µm)
Ti. Ti6Al4V (control)

Sintered Fe30Mn reference (A)

Comparing effect of adding HA to Fe30Mn (B)

Comparing 30% porosity with 50% (C–F)

Comparing leached pore sizes (C–H)

Comparing pore size and the addition of hydroxyapatite (G–H)

For reference to clinical material (Ti)

Reasons to include Hydroxyapatite ($Ca_5(PO_4)_3(OH)$**):**

- Adding HA increases mineralized extracellular matrix
- Tissue can form chemical bonds, decreasing implant loosening
- Above 900C, HA decomposes into Tricalcium Phosphate phases

Lu, J. Descamps, M. Dejou, J. Koubi, G. Harouin, P. Lemaitre J. Proust, J.P. The Biodegradation Mechanism of Calcium Phosphate Biomaterials in Bone

Powder Sizes

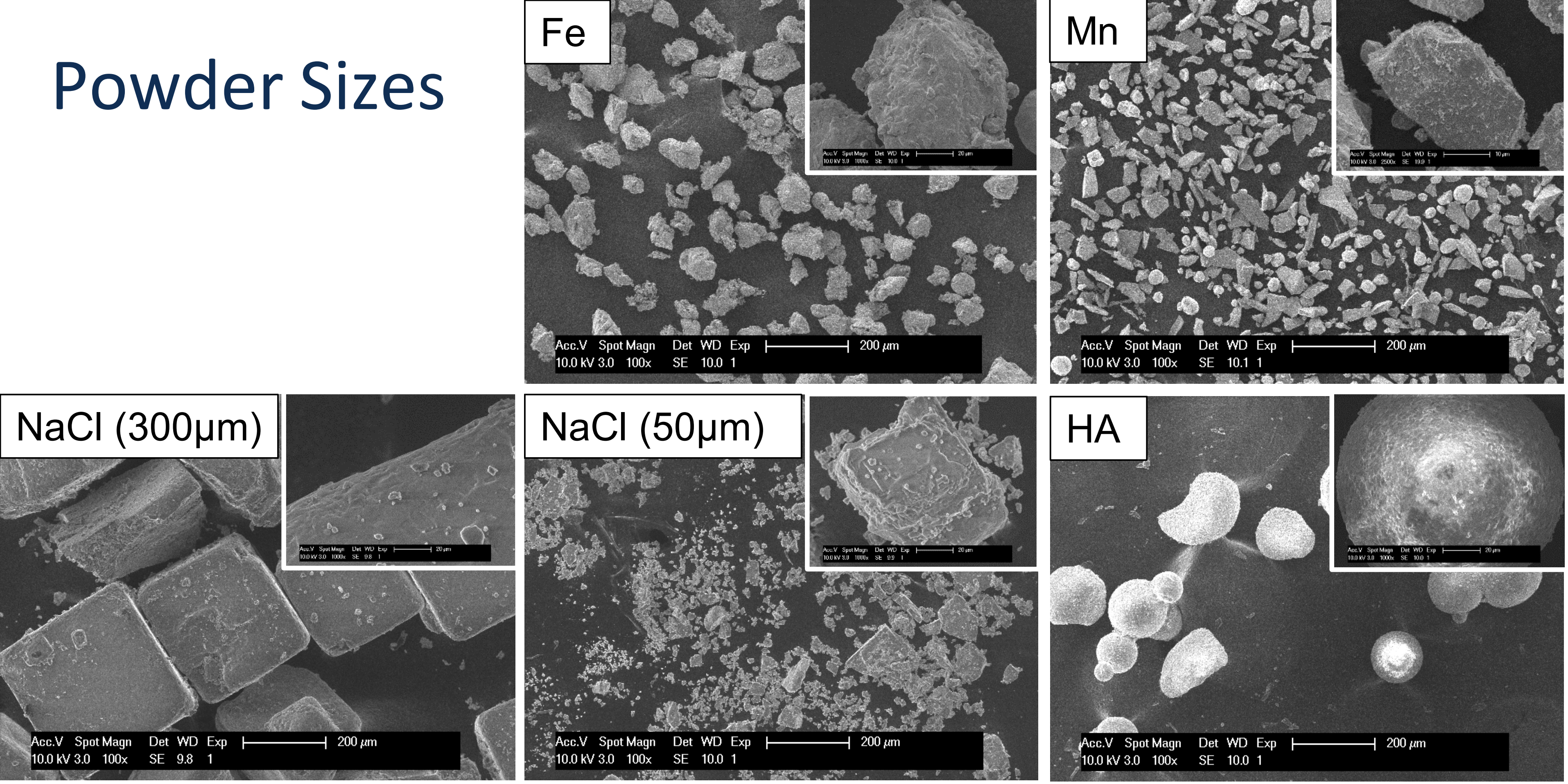

Powder	Average dia (µm)	Stdev (µm)
Fe	64.23	10.49
Mn	45.13	8.80
HA	154.03	15.18
NaCl (big)	306.07	16.34
NaCl (small)	50.51	6.28

Heiden, M. Nauman E, Johnson D, Stanciu L. Bioresorbable Fe-Mn and Fe-Mn-HA Materials for Orthopedic Implantation: Enhancing Degradation through Porosity Control, *Adv. Healthcare* 6(13),10.1002/adhm.201700120 (2017)

Mechanical Properties

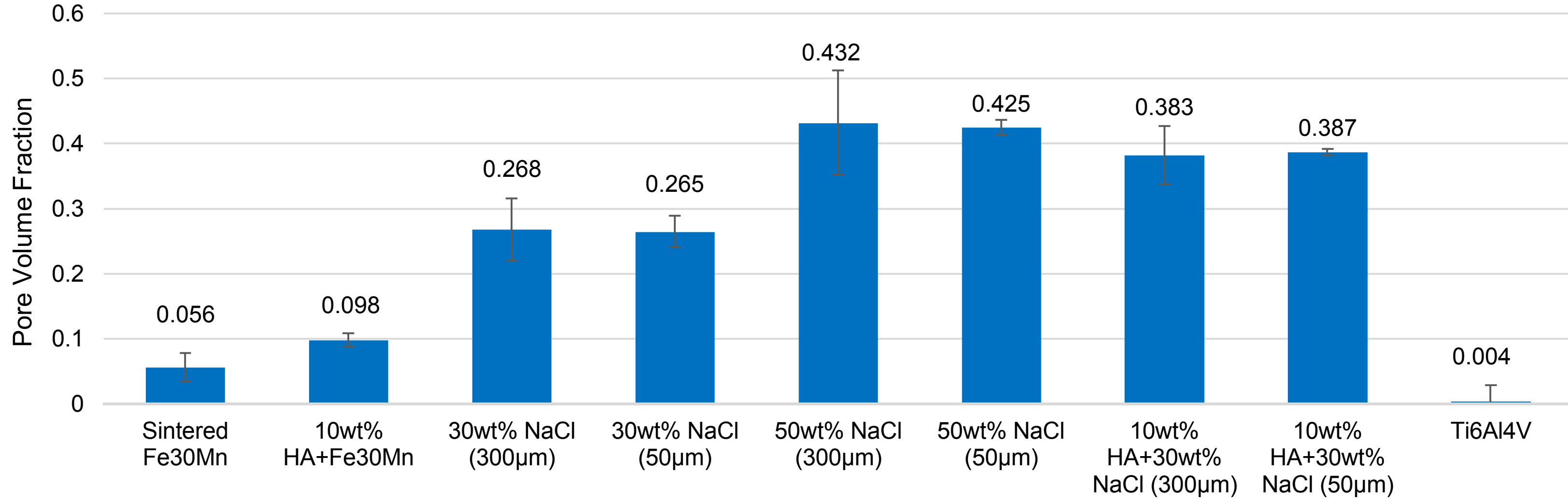

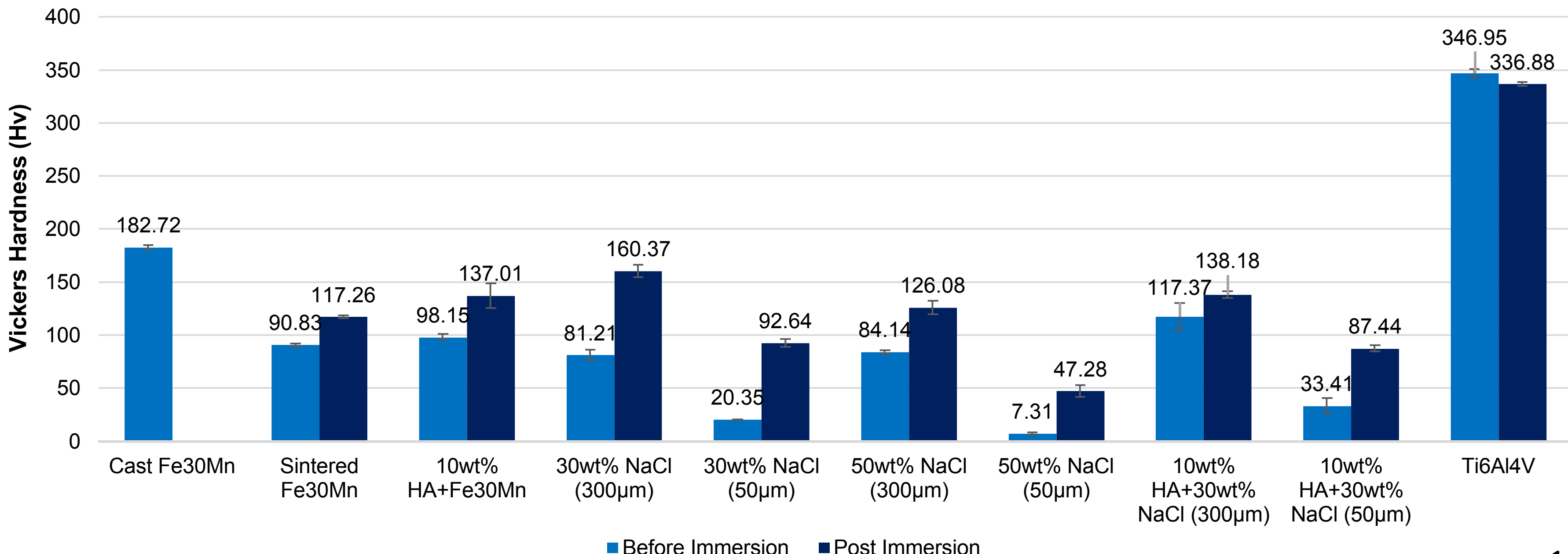

Heiden, M. Nauman E, Johnson D, Stanciu L. Bioresorbable Fe-Mn and Fe-Mn-HA Materials for Orthopedic Implantation: Enhancing Degradation through Porosity Control, *Adv. Healthcare* 6(13),10.1002/adhm.201700120 (2017)

Samples Prior to Immersion

Sandia National Laboratories

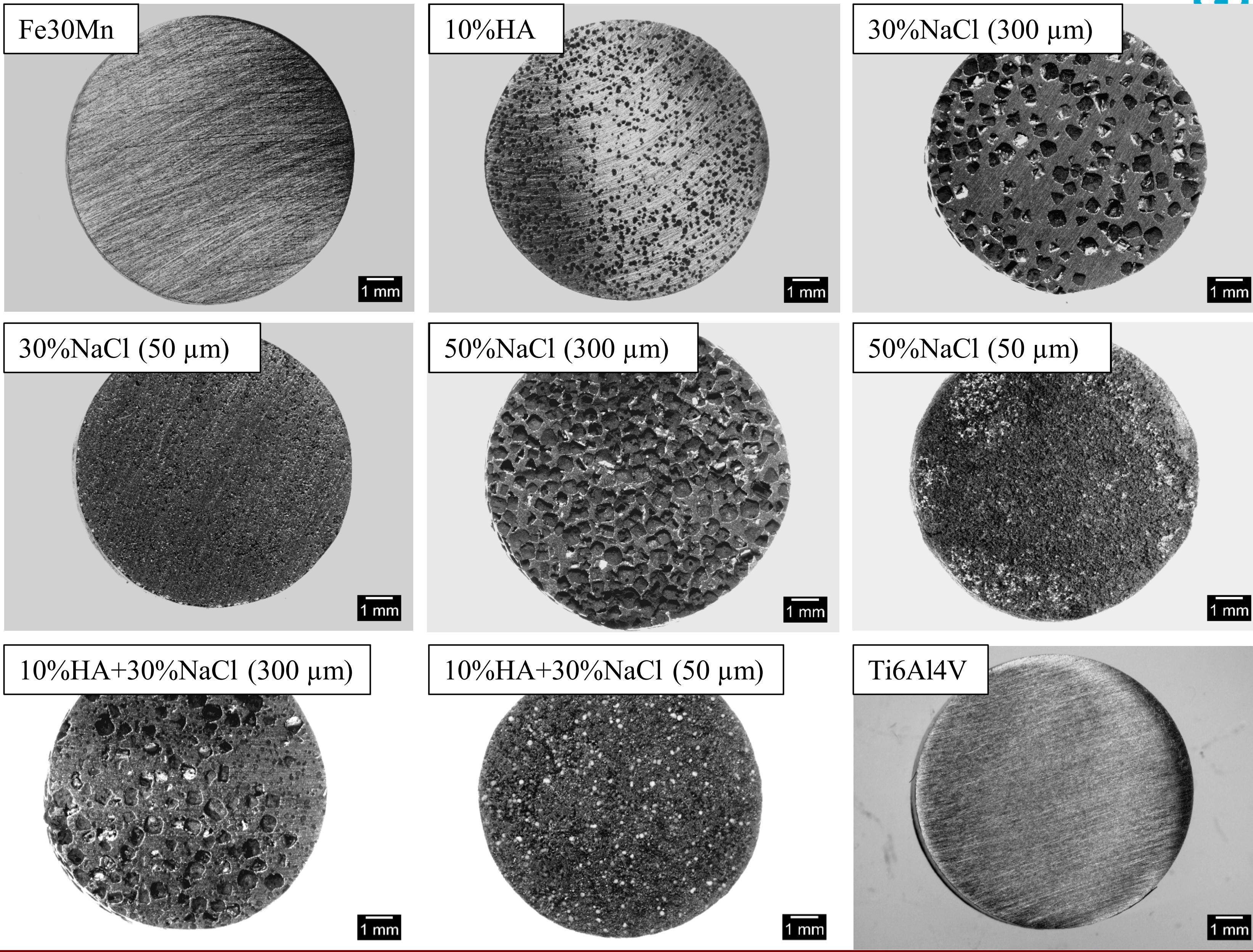

Heiden, M. Nauman E, Johnson D, Stanciu L. Bioresorbable Fe-Mn and Fe-Mn-HA Materials for Orthopedic Implantation: Enhancing Degradation through Porosity Control, *Adv. Healthcare* 6(13),10.1002/adhm.201700120 (2017)

Samples After 30 day Immersion

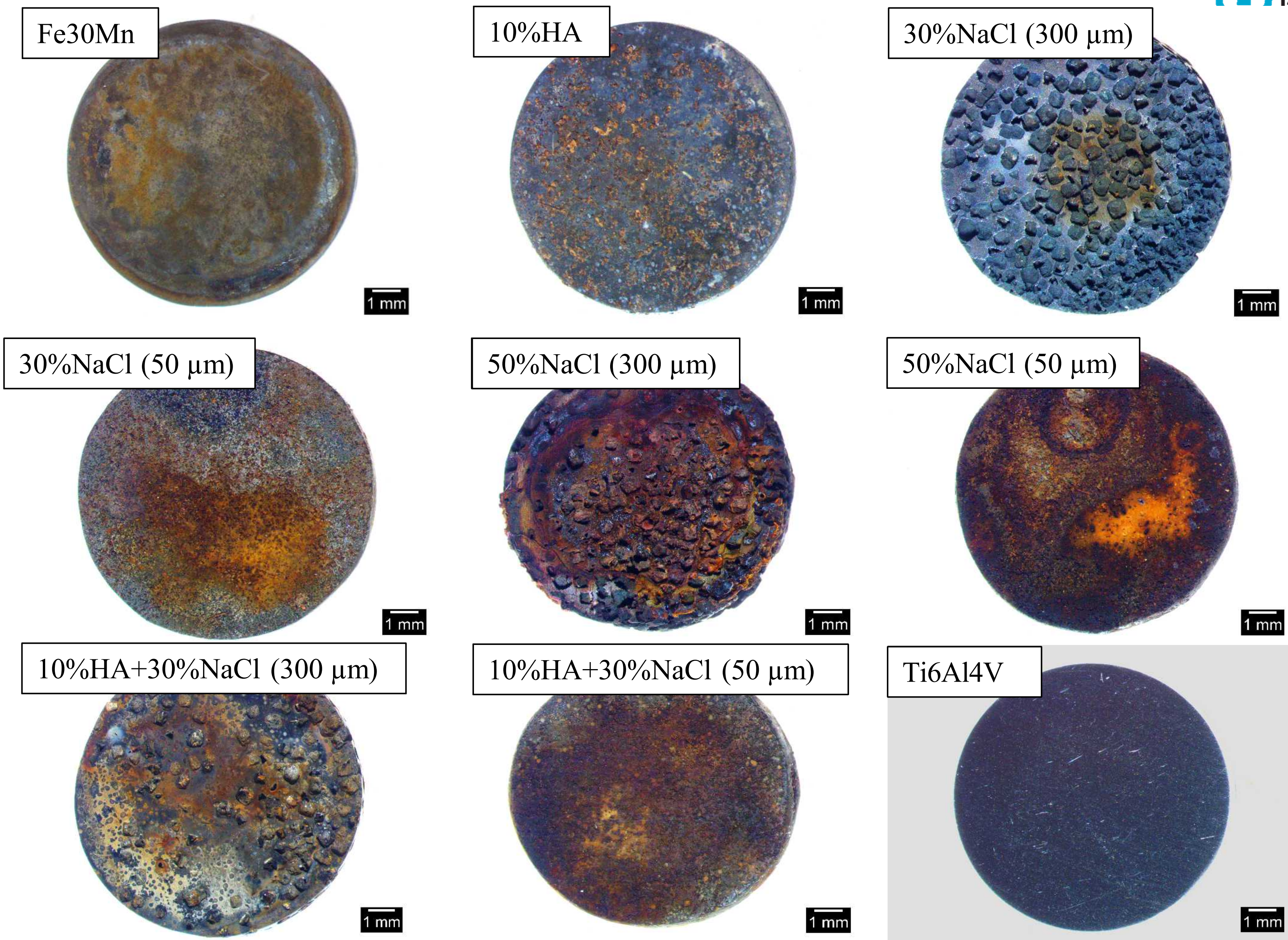

Cell attachment: Day 1 (Fluorescence)

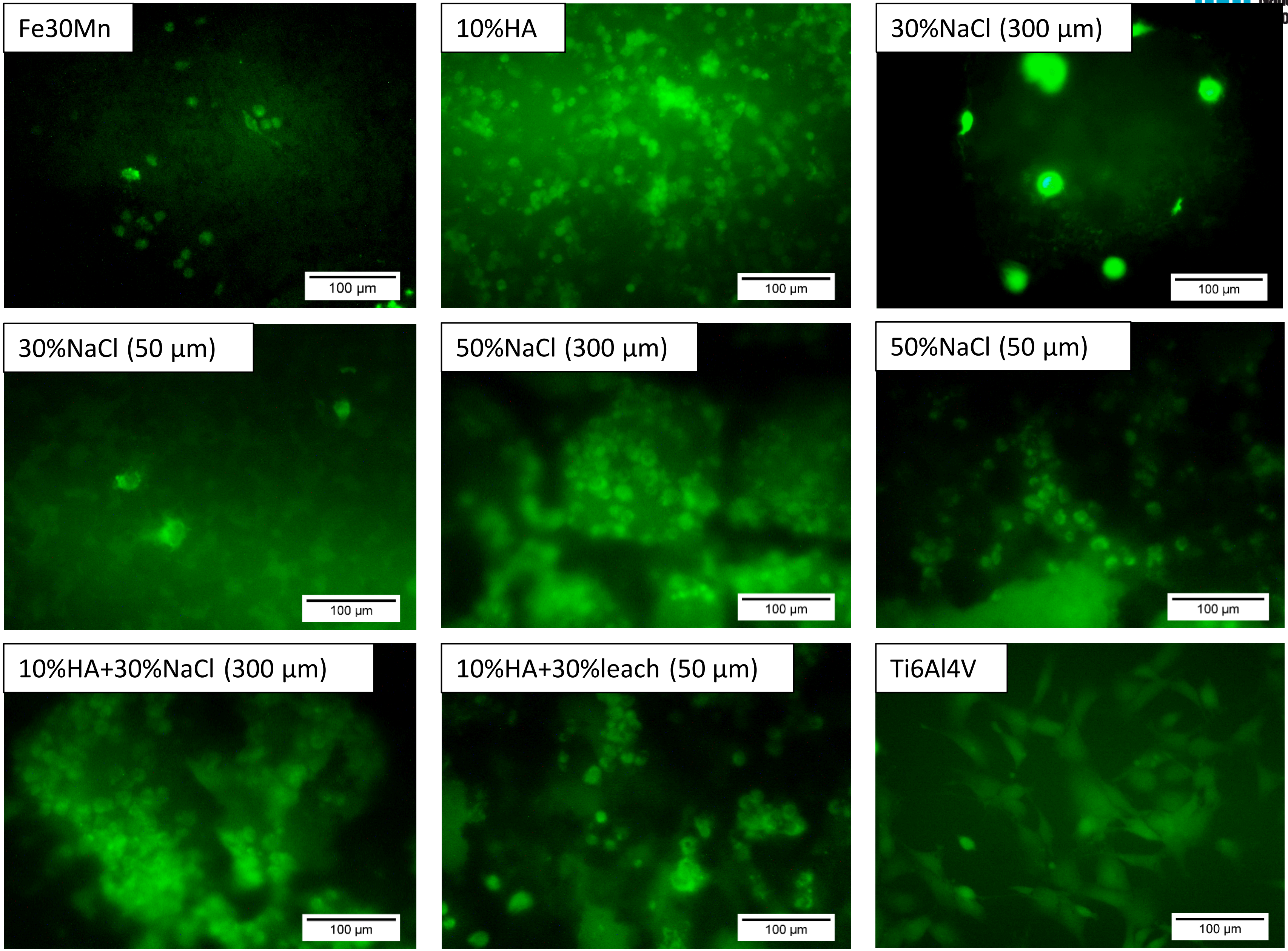

Heiden, M. Nauman E, Johnson D, Stanciu L. Bioresorbable Fe-Mn and Fe-Mn-HA Materials for Orthopedic Implantation: Enhancing Degradation through Porosity Control, *Adv. Healthcare* 6(13),10.1002/adhm.201700120 (2017)

Cell attachment: Day 30 (Fluorescence)

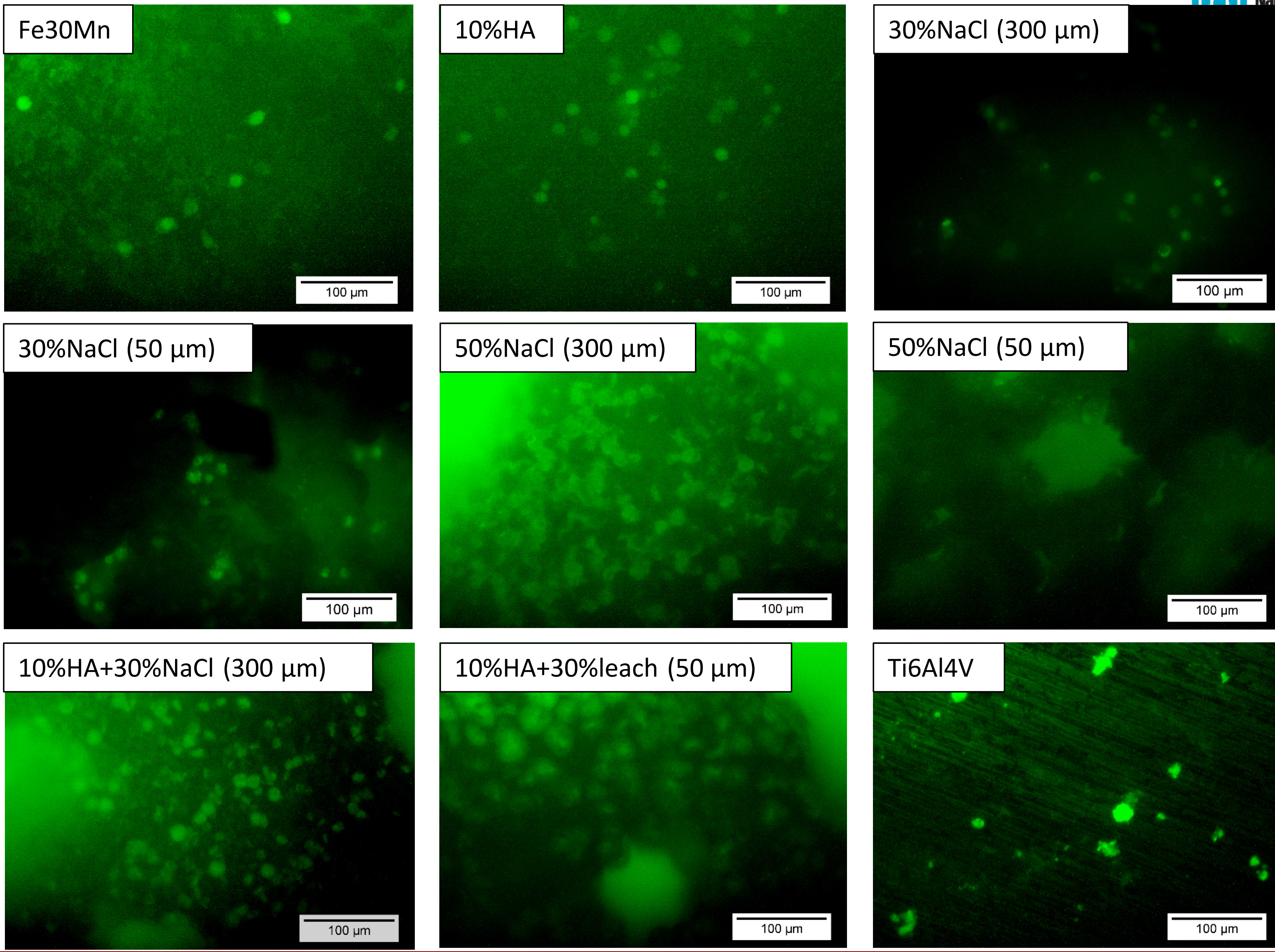

Heiden, M. Nauman E, Johnson D, Stanciu L. Bioresorbable Fe-Mn and Fe-Mn-HA Materials for Orthopedic Implantation: Enhancing Degradation through Porosity Control, *Adv. Healthcare* 6(13),10.1002/adhm.201700120 (2017)

Mechanical Properties

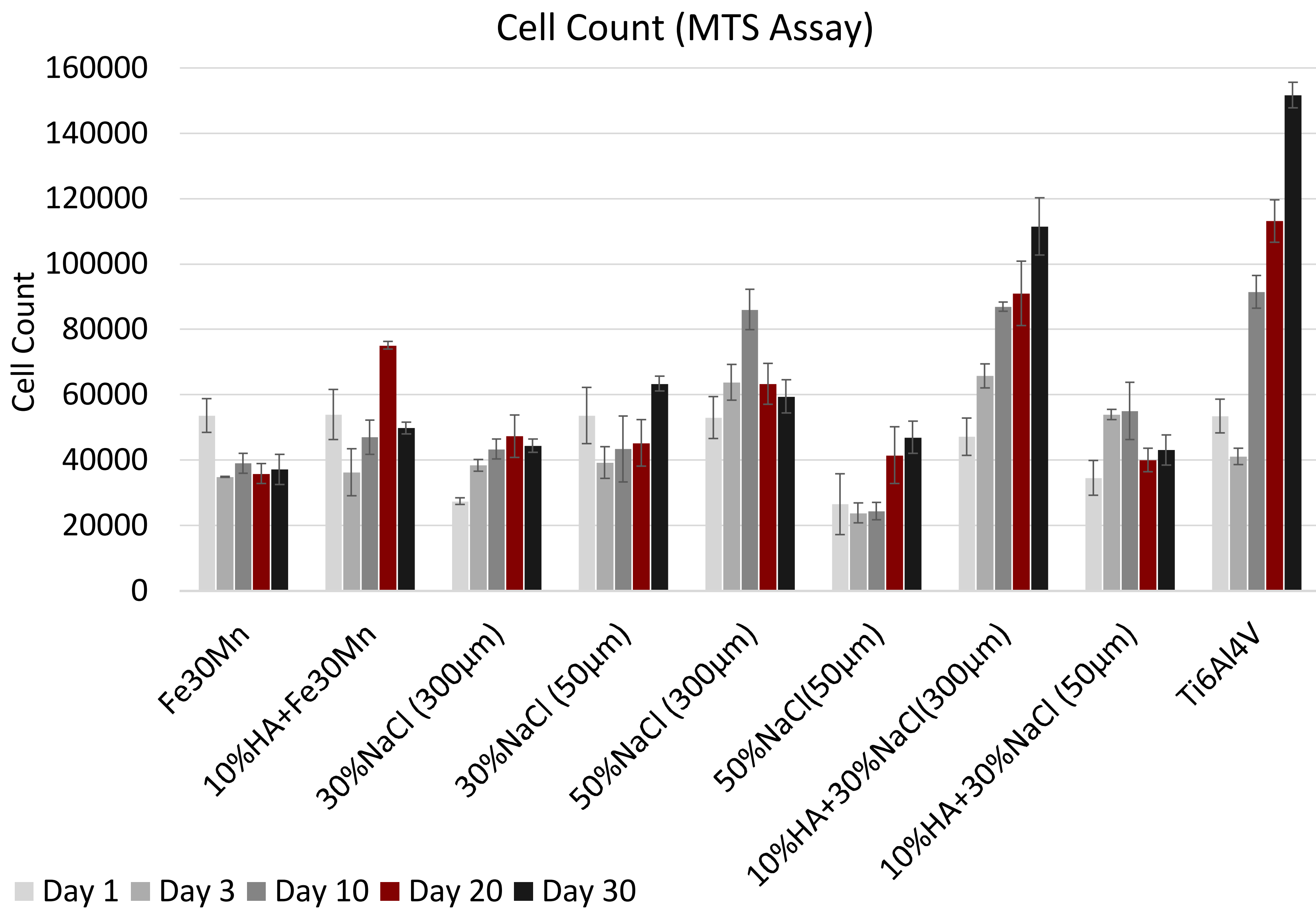

Heiden, M. Nauman E, Johnson D, Stanciu L. Bioresorbable Fe-Mn and Fe-Mn-HA Materials for Orthopedic Implantation: Enhancing Degradation through Porosity Control, *Adv. Healthcare* 6(13),10.1002/adhm.201700120 (2017)

Initial Surfaces (SEM) – 100X

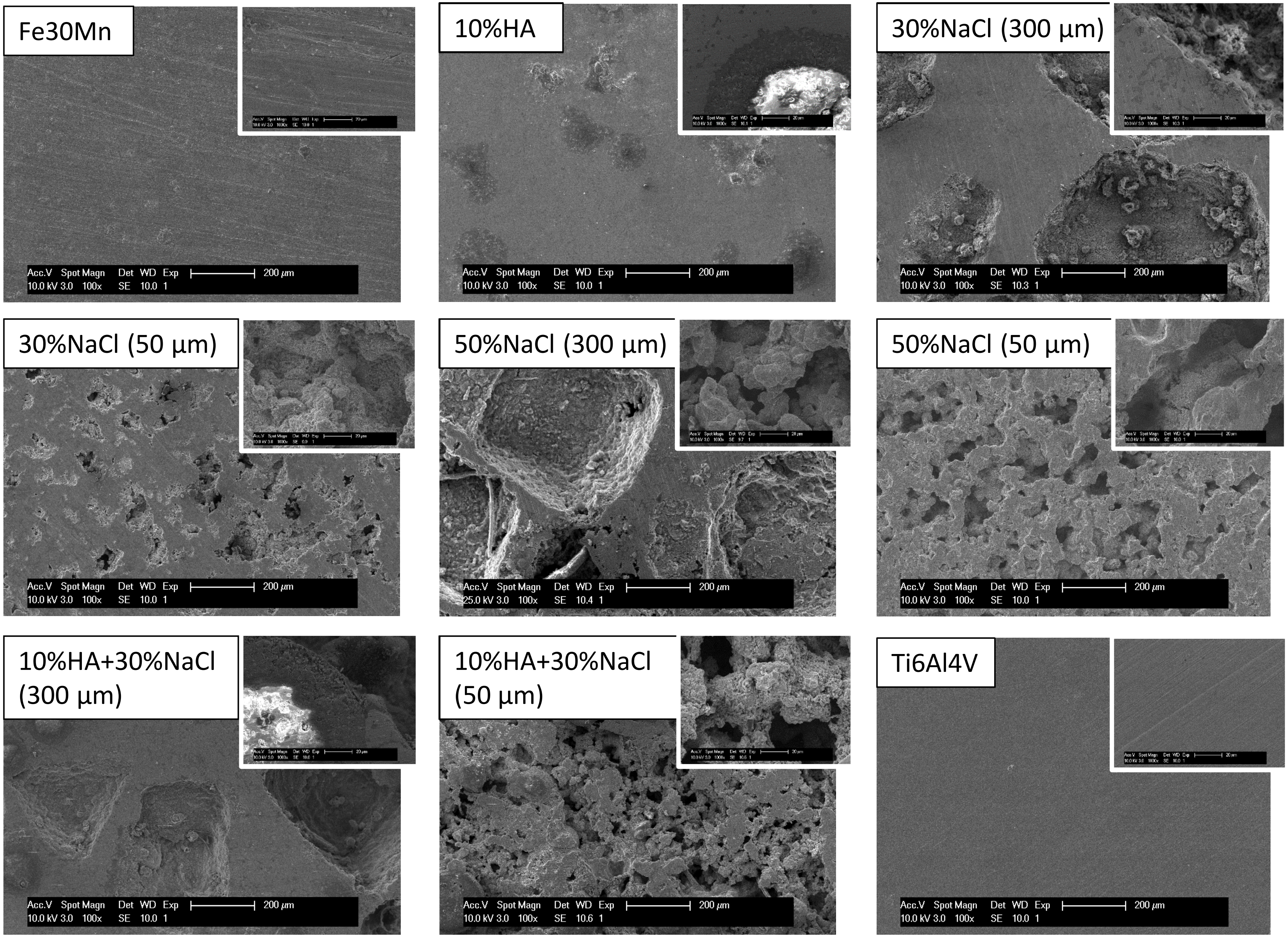

Heiden, M. Nauman E, Johnson D, Stanciu L. Bioresorbable Fe-Mn and Fe-Mn-HA Materials for Orthopedic Implantation: Enhancing Degradation through Porosity Control, *Adv. Healthcare* 6(13),10.1002/adhm.201700120 (2017)

SEM 30 days

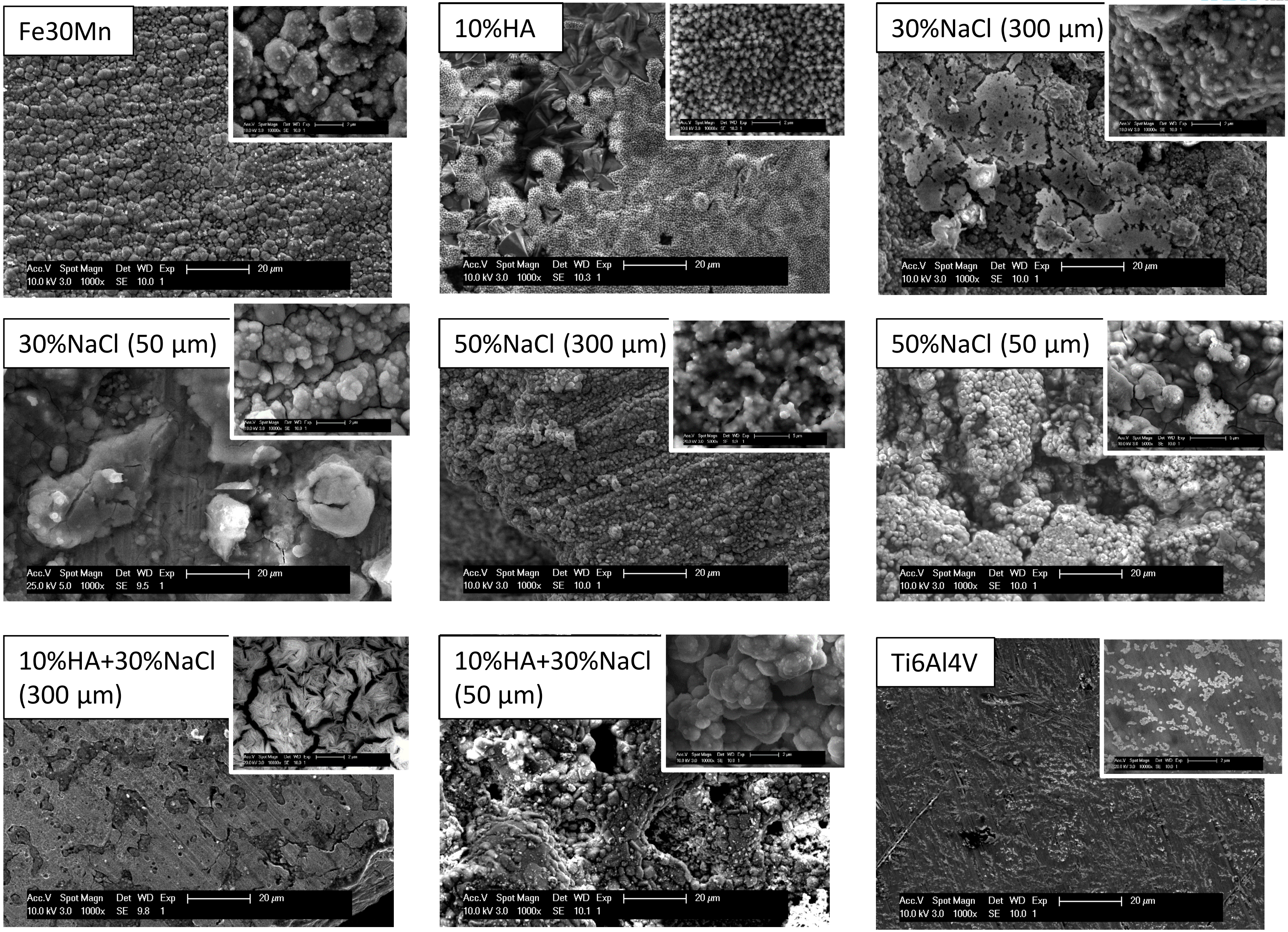

Heiden, M. Nauman E, Johnson D, Stanciu L. Bioresorbable Fe-Mn and Fe-Mn-HA Materials for Orthopedic Implantation: Enhancing Degradation through Porosity Control, *Adv. Healthcare* 6(13),10.1002/adhm.201700120 (2017)

Corrosion after 30 Days *in vitro*

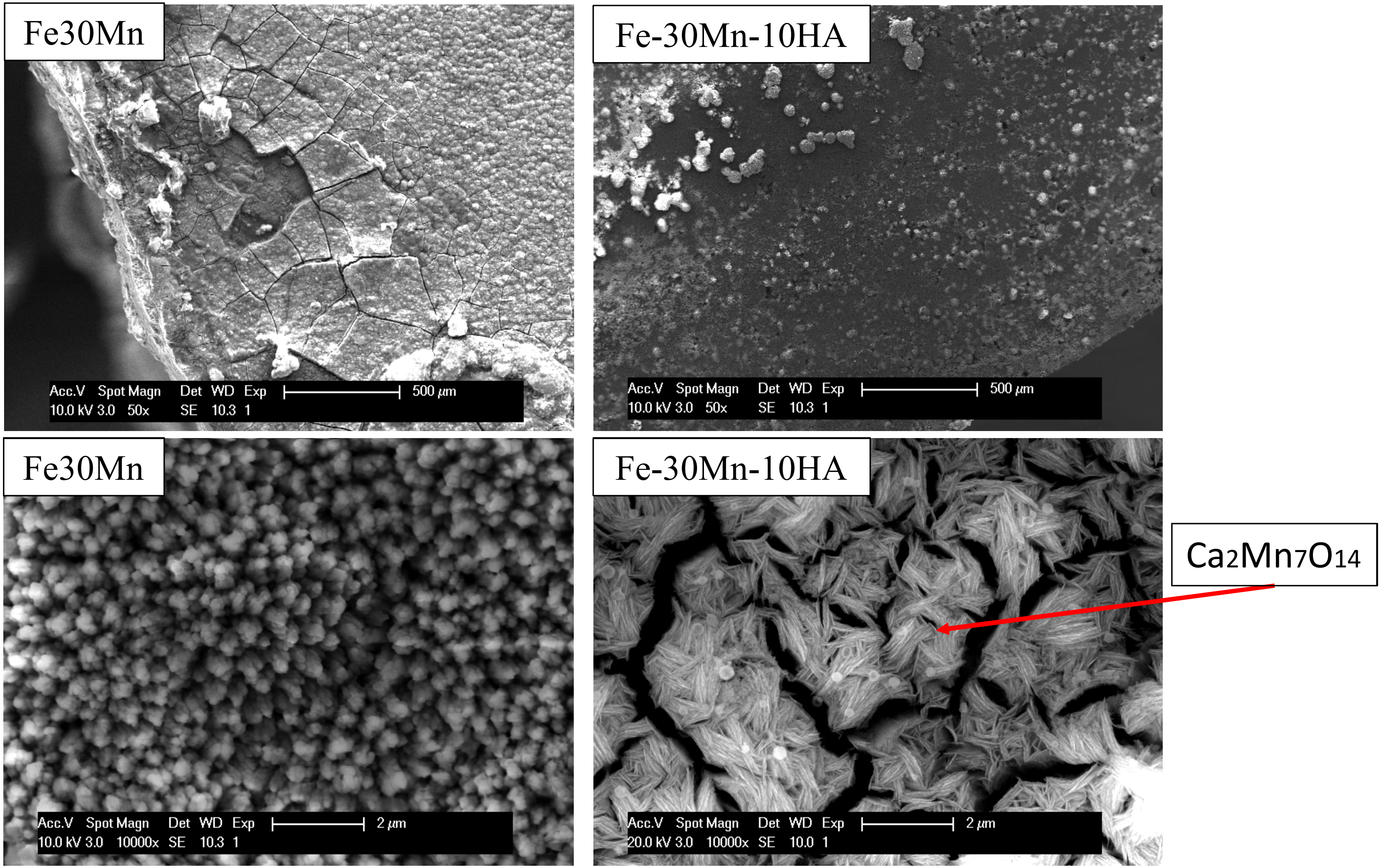

Heiden, M. Nauman E, Johnson D, Stanciu L. Bioresorbable Fe-Mn and Fe-Mn-HA Materials for Orthopedic Implantation: Enhancing Degradation through Porosity Control, *Adv. Healthcare* 6(13),10.1002/adhm.201700120 (2017)

Mechanical Properties (Continued)

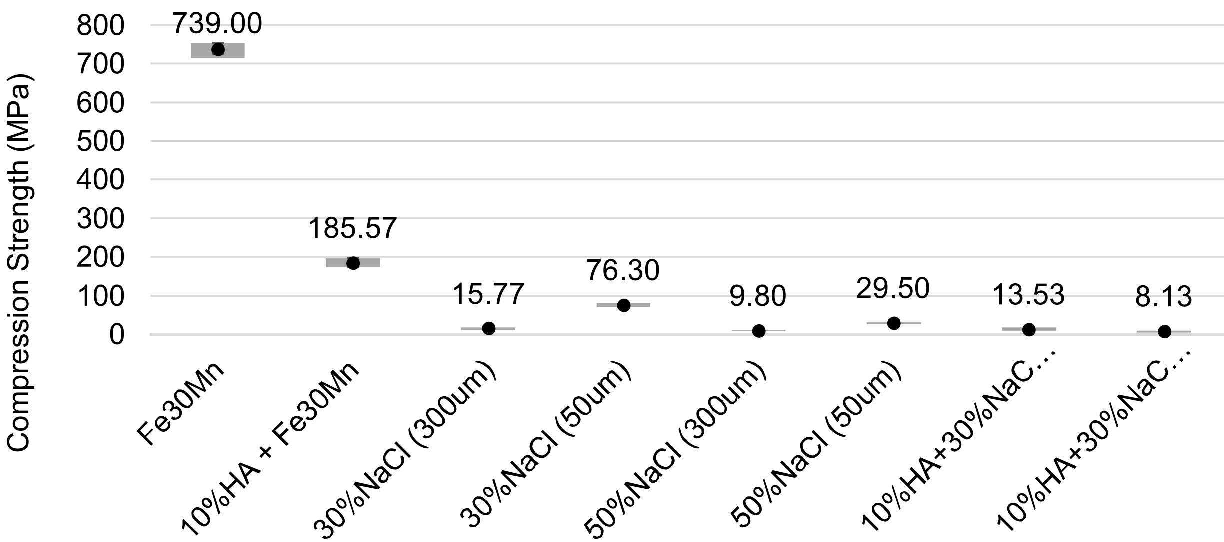

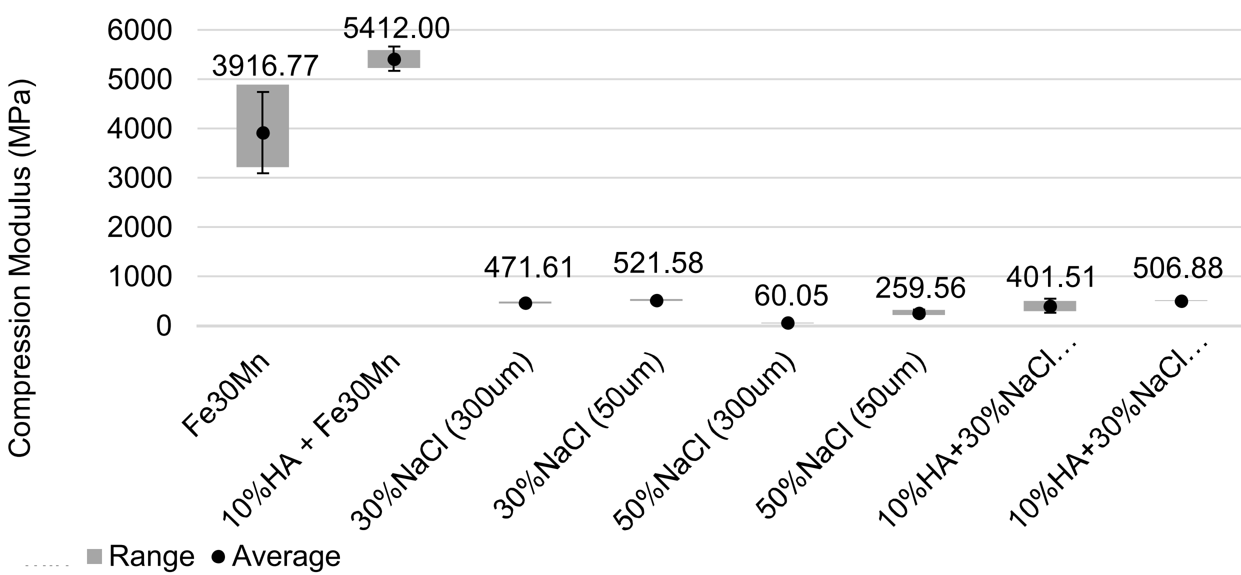

Compressive Strength:

Cancellous bone:

~2–10 MPa

316L Stainless Steel:

~240 MPa

Heiden, M. Nauman E, Johnson D, Stanciu L. Bioresorbable Fe-Mn and Fe-Mn-HA Materials for Orthopedic Implantation: Enhancing Degradation through Porosity Control, *Adv. Healthcare* 6(13),10.1002/adhm.201700120 (2017)

Apparent Corrosion Rates

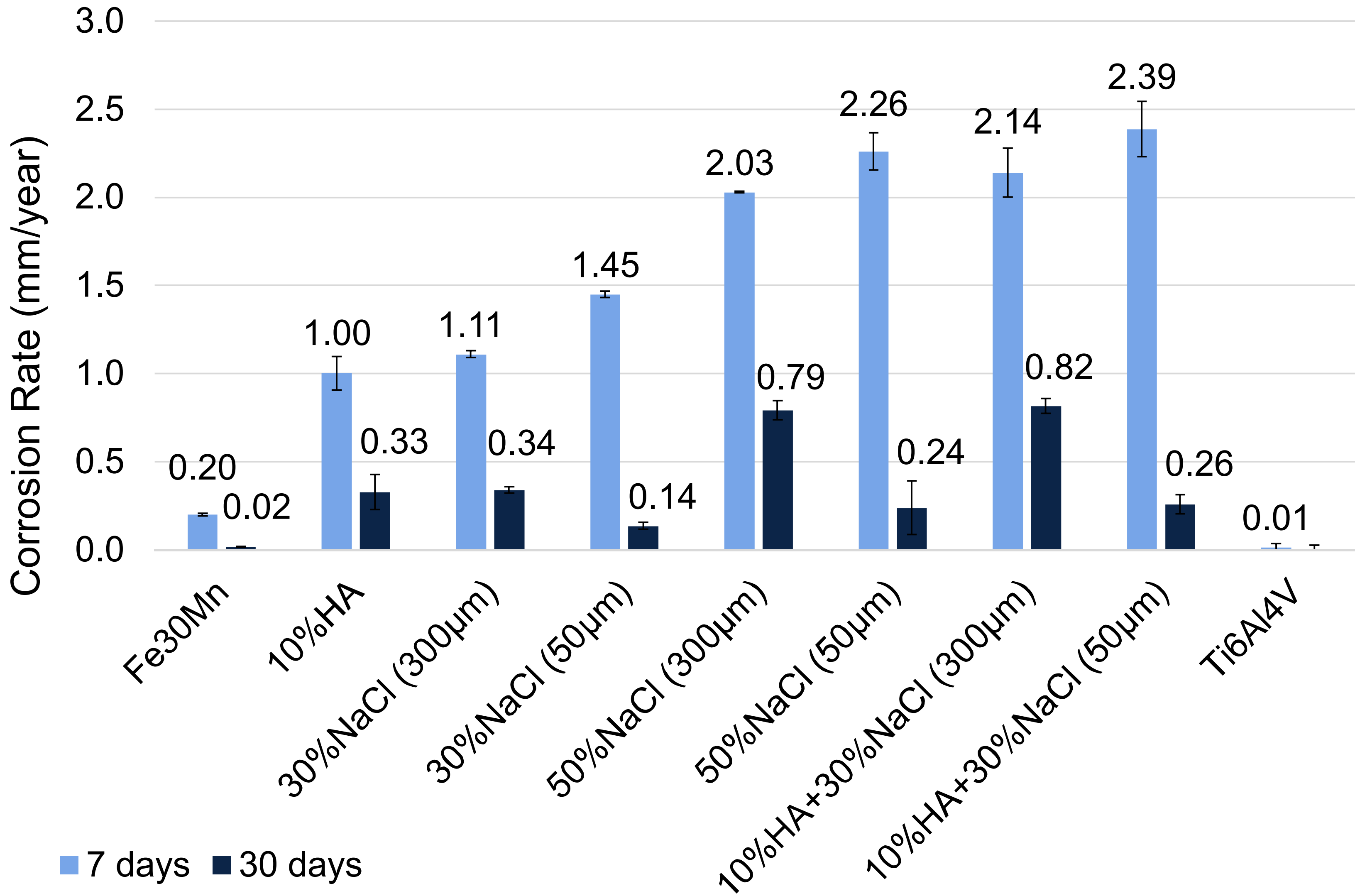

Heiden, M. Nauman E, Johnson D, Stanciu L. Bioresorbable Fe-Mn and Fe-Mn-HA Materials for Orthopedic Implantation: Enhancing Degradation through Porosity Control, *Adv. Healthcare* 6(13),10.1002/adhm.201700120 (2017)

Conclusions

- Fe-rich oxide layer initially forms on Fe-Mn surfaces
- NaCl-leaching of Fe-Mn alloys creates macropores, increases degradation & cell attachment
- Formation of Calcium Manganese Oxide ($Ca_2Mn_7O_{14}$) at 1200 C, increases corrosion
- Incorporation of HA inhibits typical flaking effect of Fe-Mn alloys

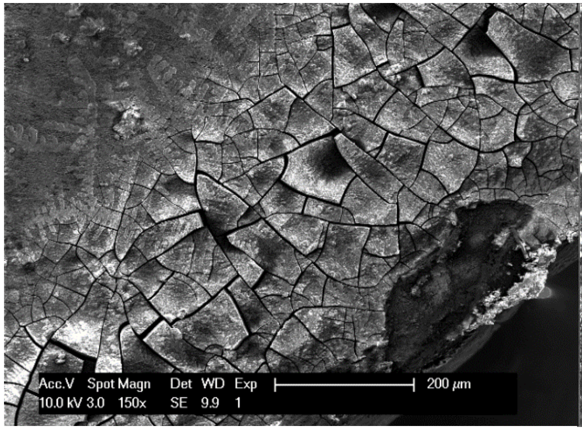

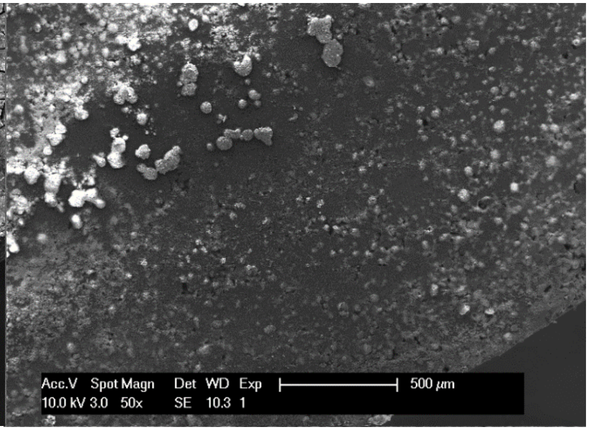

Conclusions

- Different Ca and P structures deposited on the surface post 30 day immersion
- Corrosion is generally high within the first 7 days and then steadily drops
- Larger porosity (300 µm) increased overall degradation rate after 30 days
- 10%HA + 30%NaCl (300 µm) showed the highest degradation after 30 days
- All materials except the 50% NaCl (300 µm) & 10%HA + 30%NaCl (50 µm) had compression strengths above cancellous bone (2-10 MPa)

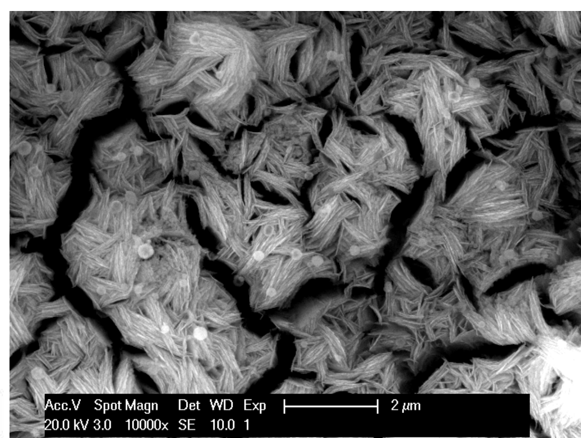

Acknowledgements

- Purdue School of Materials Engineering
- National Science Foundation
- Sabrina Huang
- Dr. Eric Nauman
- Dr. Mahdi Dehestani
- Dr. Andrew Kustas
- Dr. Kevin Chaput

*This material is based upon work supported by the National Science Foundation Graduate Research Fellowship under Grant No. DGE-1333468. Any opinion, findings, and conclusions or recommendations expressed in this material are those of the authors and do not necessarily reflect the views of the National Science Foundation.

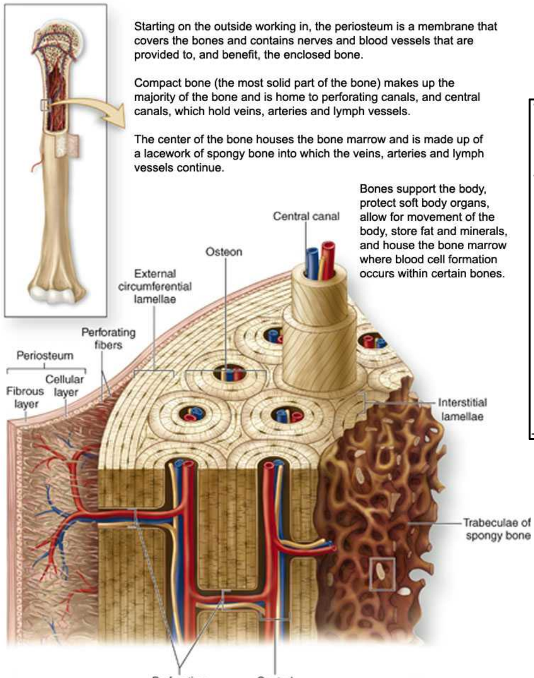

	Vol. % mineral	Porosity (%)	Pore size (μm)	ρ (g/cm^3)	σ (MPa)	E (GPa)
Cortical bone	30-40	5 – 10	10 – 50	2.0	110 – 150	18 – 22
Cancellous bone	30-40	75 – 85	300 – 600	0.2 – 0.5	2 – 6	0.1 – 0.3
Natural HA scaffolds	100	50–90	100–600	0.3–1.3	0.4–9.7	0.1–1.2
Synthetic HA scaffolds	100	50–70	10–50	0.9–1.7	0.7–95.1	0.1–19.2

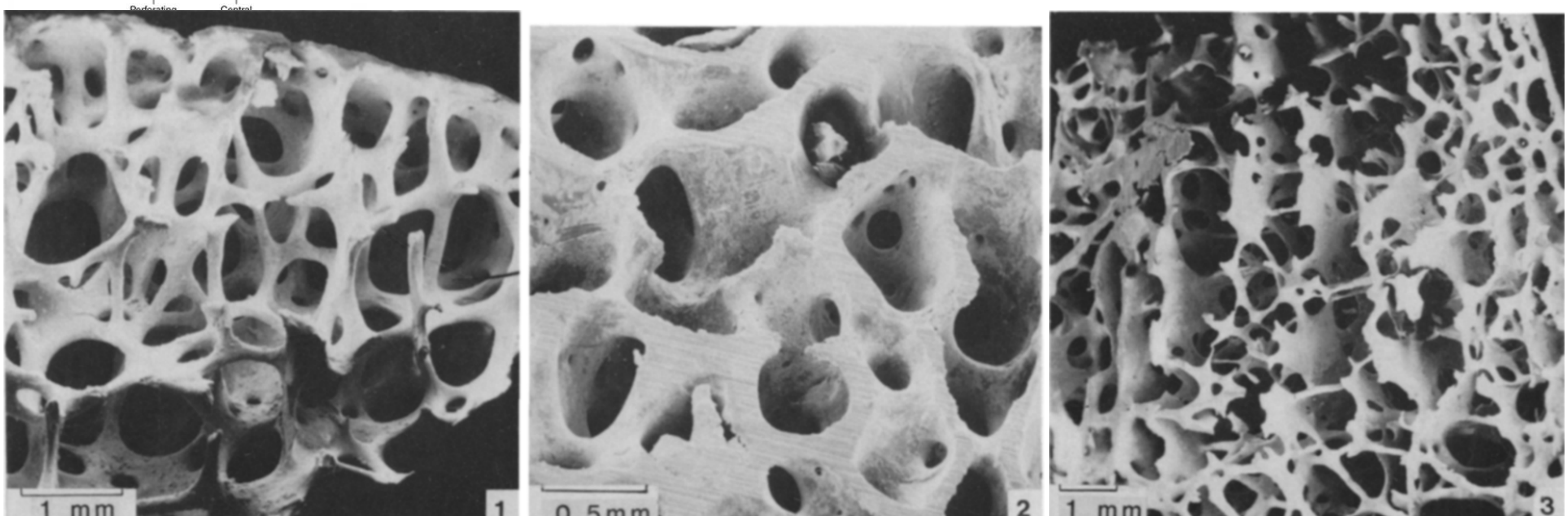

http://nutters.com/old/boneinternal.jpg

Gibson, L. . THE MECHANICAL BEHAVIOUR OF CANCELLOUS BONE. *J. Biomech.* **1985**, *18*, 317–328.

Appendix

$$CR\ (\text{mm/year}) = 3.27 \times 10^3 \left(\frac{i_{corr} \times EW}{D}\right)$$

$$\text{Corrosion rate (mm/year)} = \frac{K \times W}{A \times t \times D}$$

- Faraday's Law can be used to calculate the mass loss (m):
- $m = \frac{i*t*M}{n*F}$
- General corrosion trends can be obtained
  - Higher corrosion potential and lower current density indicates enhanced corrosion resistance
  - More negative potentials are more reactive to corrosion
  - Assumes uniform corrosion across the whole surface. It underestimates the degradation rate for when localized corrosion occurs in vivo.

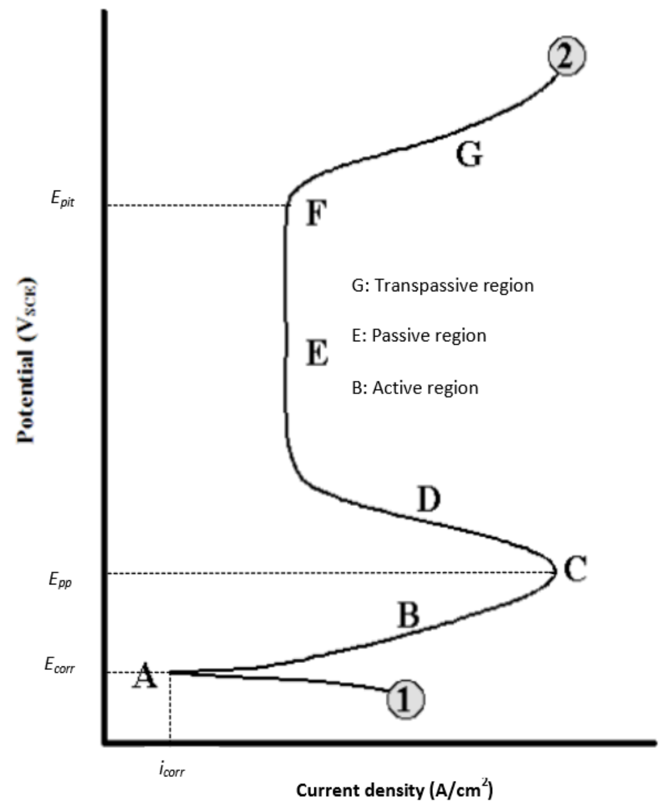

Hu, P. Improvement in Metal-on-Metal Bearing of Hip Implants with Advanced Stellite Alloys. (2013).

Mathew, M. T., Jacobs, J. J. & Wimmer, M. a. Wear-corrosion synergism in a CoCrMo hip bearing alloy is influenced by proteins. Clin. Orthop. Relat. Res. ***470,*** *3109–17 (2012).*

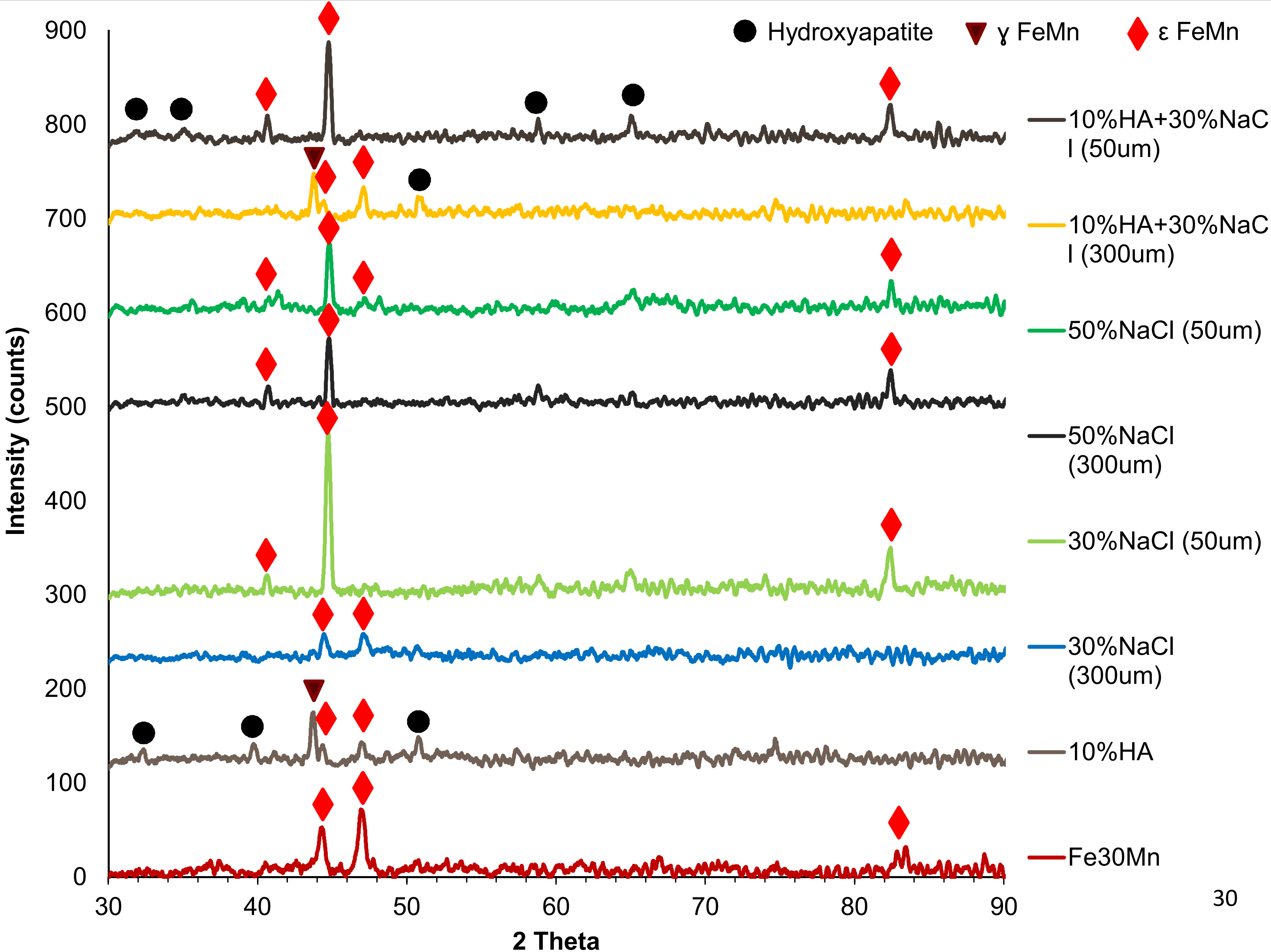
Hydroxyapatite
ɣ FeMn
ε FeMn
Intensity (counts)
900
800
700
600
500
400
300
200
100
0
30
40
50
60
70
80
90
2 Theta
10%HA+30%NaC l (50um)
10%HA+30%NaC l (300um)
50%NaCl (50um)
50%NaCl (300um)
30%NaCl (50um)
30%NaCl (300um)
10%HA
Fe30Mn

Table 2. EDS Composition Comparison

Alloy	Analyzed Compositions (wt%)						
	Fe	Mn	Ca	P	Na	Cl	O
Fe30Mn initial	70.58	29.42	-	-	-	-	-
After	42.50	28.99	9.65	11.14	0.00	2.35	5.38
10%HA initial	59.90	30.97	3.52	2.63	-	-	2.88
After	51.80	27.82	11.18	4.97	0.28	0.00	3.96
30%NaCl (300um) initial	66.9	29.61	-	-	-	-	3.49
After	58.70	27.27	4.86	7.42	0.00	0.00	1.75
30%NaCl (50um) initial	68.2	30.27	-	-	-	-	1.53
After	53.12	**32.65**	9.02	4.00	0.00	0.00	1.21
50%NaCl (300um) initial	67.40	30.61	-	-	-	-	1.99
After	46.54	14.56	11.14	15.14	4.17	1.71	6.75
50%NaCl (50um) initial	66.66	32.16	-	-	-	-	1.18
After	41.56	**39.99**	7.51	3.79	0.81	1.54	4.79
10%HA+30%NaCl (300μm) initial	55.71	28.43	8.97	6.00	-	-	0.88
After	37.26	24.30	21.56	5.99	1.83	1.70	7.36
10%HA+30%NaCl (50μm) initial	50.37	27.22	11.33	8.53	-	-	2.55
After	34.91	**48.33**	6.49	5.39	0.72	0.77	3.37
	Ti	**Al**	**V**	**O**			
Ti6Al4V initial	89.63	7.31	2.06	-	-	-	-
After	90.60	4.48	2.61	2.31	-	-	-

10% HA + Fe30Mn sintered @1200°C – 3hr

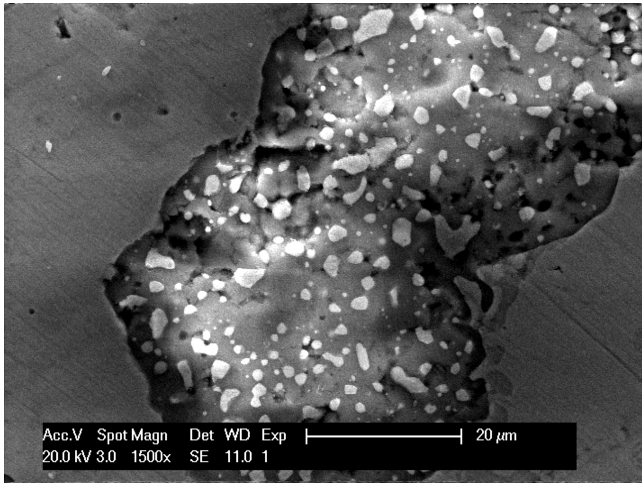

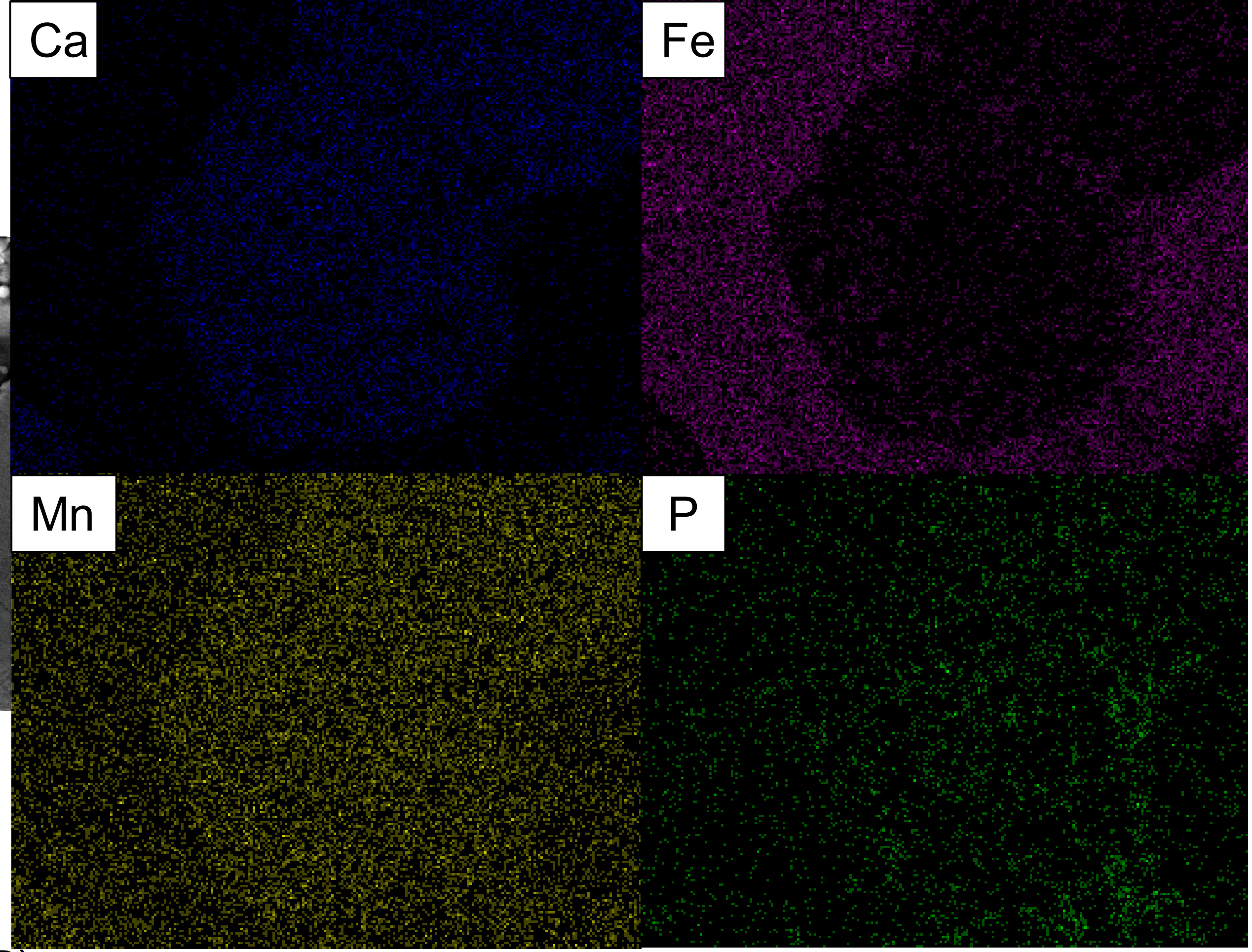

$Ca_{10}(PO_4)_6(OH)_2$

Tricalcium Phosphate (TCP)

- Adding hydroxyapatite (HAp) may increase rates of cell proliferation
- Tissue can infiltrate HAp and form chemical bonds with natural bone
- Above 1100C (2hr) it decomposes from HAp into Tricalcium Phosphate phases.
- Ca and Mn elements combine into **Calcium Manganese Oxide ($Ca_2Mn_7O_{14}$)**

Bone Mineralization (Red Alizarin Stain)